SIAM J. SCI. COMPUT.
Vol. 42, No. 6, pp. A4017–A4045

$\mathcal{H}_2$-OPTIMAL MODEL REDUCTION USING PROJECTED NONLINEAR LEAST SQUARES*

JEFFREY M. HOKANSON† AND CALEB C. MAGRUDER‡

Abstract. In many applications throughout science and engineering, model reduction plays an important role replacing expensive large-scale linear dynamical systems by inexpensive reduced order models that capture key features of the original, full order model. One approach to model reduction finds reduced order models that are locally optimal approximations in the $\mathcal{H}_2$-norm, an approach taken by the iterative rational Krylov algorithm (IRKA), among others. Here we introduce a new approach for $\mathcal{H}_2$-optimal model reduction using the projected nonlinear least squares framework previously introduced in [J. M. Hokanson, *SIAM J. Sci. Comput.*, 39 (2017), pp. A3107–A3128]. At each iteration, we project the $\mathcal{H}_2$ optimization problem onto a finite-dimensional subspace yielding a weighted least squares rational approximation problem. Subsequent iterations append this subspace such that the least squares rational approximant asymptotically satisfies the first order necessary conditions of the original, $\mathcal{H}_2$ optimization problem. This enables us to build reduced order models with similar error in the $\mathcal{H}_2$-norm but using far fewer evaluations of the expensive, full order model compared to competing methods. Moreover, our new algorithm only requires access to the transfer function of the full order model, unlike IRKA, which requires a state-space representation, or TF-IRKA, which requires both the transfer function and its derivative. Applying the projected nonlinear least squares framework to the $\mathcal{H}_2$-optimal model reduction problem opens new avenues for related model reduction problems.

Key words. model reduction, $\mathcal{H}_2$ approximation, projected nonlinear least squares, rational approximation, transfer function

AMS subject classifications. 41A20, 46E22, 90C53, 93A15, 93C05, 93C15

DOI. 10.1137/19M1247863

1. Introduction.

Model reduction replaces an expensive, high-fidelity simulation with a low-dimensional, inexpensive surrogate. Although the cost of building this *reduced order model* (ROM) is often comparable to simulating of the original *full order model* (FOM), this cost is justified in two settings: many-query settings, such as optimization and uncertainty quantification, and real-time applications where the full order simulation is unaffordable. There are a wide variety of approaches for model reduction, such as balanced truncation, proper orthogonal decomposition, and interpolatory methods; for an extensive overview, see [11]. In this paper, we address the $\mathcal{H}_2$-optimal model reduction problem—a model reduction approach requiring both the full and reduced order models to be described by a stable, linear, time-invariant dynamical system. In this setting, the action of these models is completely defined through either their *impulse response* h or their *transfer function* H, the Laplace transform of h. Under these assumptions, the transfer function H is an element of the $\mathcal{H}_2$ Hilbert space: the space of functions analytic in the closed right half plane along with the inner product

*Submitted to the journal's Methods and Algorithms for Scientific Computing section March 4, 2019; accepted for publication (in revised form) August 21, 2020; published electronically December 17, 2020.

https://doi.org/10.1137/19M1247863

Funding: The work of the first author was partially supported by DARPA's program Enabling Quantification of Uncertainty in Physical Systems (EQUiPS).

†Department of Computer Science, University of Colorado Boulder, Boulder, CO 80309 USA (Jeffrey.Hokanson@colorado.edu).

‡The MathWorks Inc., Natick, MA 01760-2098 USA (ccmagruder@gmail.com).

$$\langle F, G\rangle_{\mathcal{H}_2} \coloneqq \frac{1}{2\pi}\int_{-\infty}^{\infty} \overline{F(\mathrm{i}\omega)}G(\mathrm{i}\omega)\,\mathrm{d}w, \quad F, G \in \mathcal{H}_2, \quad \mathrm{i} \coloneqq \sqrt{-1}. \tag{1.1}$$

Given a space of candidate reduced order models whose transfer functions are in the set $\mathcal{S} \subset \mathcal{H}_2$, the goal of $\mathcal{H}_2$-optimal model reduction is to find the element $H_r \in \mathcal{S}$ that is closest to the transfer function of the full order model H in the $\mathcal{H}_2$-norm

$$\min_{H_r \in \mathcal{S}} \|H - H_r\|_{\mathcal{H}_2}^2, \quad \text{where} \quad \|F\|_{\mathcal{H}_2}^2 \coloneqq \langle F, F\rangle_{\mathcal{H}_2}. \tag{1.2}$$

As we consider a case where $\mathcal{S}$ is nonconvex, we consider local optimizers satisfying the first order optimality conditions as solutions to (1.2).

Here we employ the *projected nonlinear least squares framework* introduced by Hokanson [31] to solve the $\mathcal{H}_2$-optimal model reduction problem (1.2). This framework replaces (1.2) by a sequence of small, finite-dimensional *projected problems* whose optimizers converge to an optimizer of (1.2). Each projected problem introduces an orthogonal projector $P(\boldsymbol{\mu})$ into the norm, solving

$$\min_{H_r \in \mathcal{S}} \|P(\boldsymbol{\mu})[H - H_r]\|_{\mathcal{H}_2}^2. \tag{1.3}$$

Exploiting the *reproducing kernel* structure of $\mathcal{H}_2$ (see the discussion in subsection 2.2), we construct these projectors using kernel vectors $v[\mu] \in \mathcal{H}_2$ where $\langle v[\mu], F\rangle_{\mathcal{H}_2} = F(\mu)$ such that the range of $P(\boldsymbol{\mu})$ is spanned by $\{v[\mu_j]\}_{j=1}^n$. This allows the objective of (1.3) to be rewritten as a weighted least squares problem involving the mismatch $H - H_r$ evaluated at the *interpolation points* $\boldsymbol{\mu} = [\mu_1, \ldots, \mu_n]$,

$$\|P(\boldsymbol{\mu})(H - H_r)\|_{\mathcal{H}_2}^2 = \left\| \mathbf{M}(\boldsymbol{\mu})^{-\frac{1}{2}} \left(\begin{bmatrix} H(\mu_1) \\ \vdots \\ H(\mu_n) \end{bmatrix} - \begin{bmatrix} H_r(\mu_1) \\ \vdots \\ H_r(\mu_n) \end{bmatrix} \right) \right\|_2^2, \tag{1.4}$$

where $\mathbf{M}(\boldsymbol{\mu})$ is a Gram matrix of the kernel vectors $v[\mu_j]$ acting to preserve the norm; i.e., $[\mathbf{M}(\boldsymbol{\mu})]_{j,k} = \langle v[\mu_j], v[\mu_k]\rangle_{\mathcal{H}_2}$ with explicit definition in (4.7). As the projected problem is a finite-dimensional nonlinear least squares problem, we can find local minimizers of (1.3) using standard optimization techniques given a parameterization of $\mathcal{S}$; we refer to this as *inner loop*.

Around this inner loop we construct an *outer loop* updating the projector $P(\boldsymbol{\mu})$ such that local optimizers of the projected problem (1.3) converge to a local optimizer of the original problem (1.2). The following lemma provides the key insight connecting local optimizers of these two problems.

LEMMA 1.1. *Suppose $\mathcal{S} \subset \mathcal{H}_2$ admits a parameterization by $H_r(\cdot;\boldsymbol{\theta})$ such that $\mathcal{S} = \{H_r(\cdot;\boldsymbol{\theta}) : \boldsymbol{\theta} \in \mathcal{D}\}$ and $\mathcal{D} \subset \mathbb{R}^p$ is open. Let $\mathcal{T}(\boldsymbol{\theta})$ denote subspace containing the derivatives of H_r with respect to this parameterization at $\boldsymbol{\theta}$,*

$$\mathcal{T}(\boldsymbol{\theta}) \coloneqq \operatorname{Span}\left\{ \tfrac{\partial H_r(\cdot,\boldsymbol{\theta})}{\partial \theta_1}, \ldots, \tfrac{\partial H_r(\cdot,\boldsymbol{\theta})}{\partial \theta_p} \right\}. \tag{1.5}$$

If $H_r(\cdot, \widehat{\boldsymbol{\theta}})$ is a local optimizer of the projected problem (1.3) *and* $\operatorname{Range} P(\boldsymbol{\mu}) \supseteq \mathcal{T}(\widehat{\boldsymbol{\theta}})$, *then $H_r(\cdot, \widehat{\boldsymbol{\theta}})$ is also a local optimizer of the original problem* (1.2).

Proof. If $H_r(\cdot, \widehat{\boldsymbol{\theta}}) \in \mathcal{M}$ is a local optimizer of the projected (1.3) problem, then

$$\langle P(\boldsymbol{\mu})[H - H_r(\cdot, \widehat{\boldsymbol{\theta}})], T\rangle_{\mathcal{H}_2} = 0 \quad \forall T \in \mathcal{T}(\widehat{\boldsymbol{\theta}}). \tag{1.6}$$

As $P(\boldsymbol{\mu})$ is an orthogonal projector we can move it into the right argument and noting $P(\boldsymbol{\mu})T = T$ since, by assumption, $\mathcal{T}(\widehat{\boldsymbol{\theta}}) \subseteq \operatorname{Range} P(\boldsymbol{\mu})$, we have

$$\langle P(\boldsymbol{\mu})[H - H_r(\cdot, \widehat{\boldsymbol{\theta}})], T\rangle_{\mathcal{H}_2} = \langle H - H_r(\cdot, \widehat{\boldsymbol{\theta}}), P(\boldsymbol{\mu})T\rangle_{\mathcal{H}_2} = \langle H - H_r(\cdot, \widehat{\boldsymbol{\theta}}), T\rangle_{\mathcal{H}_2}. \tag{1.7}$$

Thus $H(\cdot, \widehat{\boldsymbol{\theta}})$ is a local optimizer of the original problem (1.8) since

$$\langle H - H_r(\cdot, \widehat{\boldsymbol{\theta}}), T\rangle_{\mathcal{H}_2} = 0 \quad \forall T \in \mathcal{T}(\widehat{\boldsymbol{\theta}}). \tag{1.8}$$

∎

Motivated by this insight, we design the outer loop to increase the range of the projector $P(\boldsymbol{\mu})$ such that (asymptotically) we satisfy the containment requirement of Lemma 1.1. To recycle existing evaluations of the transfer function, each iteration of the outer loop adds an interpolation point to the projector, i.e.,

$$\boldsymbol{\mu}^+ = [\mu_1, \ldots, \mu_n, \mu_{n+1}] \quad \Longrightarrow \quad \operatorname{Range} P(\boldsymbol{\mu}) \subset \operatorname{Range} P(\boldsymbol{\mu}^+). \tag{1.9}$$

1.1. Space of reduced order models. Although the projected nonlinear least squares framework can be applied to any family of reduced order models $\mathcal{S}$ with a finite-dimensional parameterization, the details of both the inner and the outer loop depend on this choice. Due to their popularity, here we restrict our attention to state-space reduced order models posed over the field $\mathbb{F}$ that is either real $\mathbb{R}$ or complex $\mathbb{C}$,

$$\left.\begin{cases} \mathbf{x}_r'(t) = \mathbf{A}_r\mathbf{x}_r(t) + \mathbf{b}_r u(t), \quad \mathbf{x}_r(0) = \mathbf{0} \\ y_r(t) = \mathbf{c}_r^*\mathbf{x}_r(t) \end{cases}\right\}, \quad \text{where} \quad \mathbf{A}_r \in \mathbb{F}^{r\times r},\ \mathbf{b}_r, \mathbf{c}_r \in \mathbb{F}^r, \tag{1.10}$$

and whose transfer function is

$$H_r(z; \mathbf{A}_r, \mathbf{b}_r, \mathbf{c}_r) \coloneqq \mathbf{c}_r^*[z\mathbf{I} - \mathbf{A}_r]^{-1}\mathbf{b}_r. \tag{1.11}$$

This transfer function is a degree $(r-1, r)$ rational function as the resolvent $[z\mathbf{I}-\mathbf{A}_r]^{-1}$ is a degree $(r-1, r)$ matrix-valued rational function [34, Chap. 1, eq. (5.23)]. We denote the space of $(r-1, r)$ scalar-valued rational functions as

$$\mathcal{R}_r(\mathbb{F}) \coloneqq \left\{ \frac{p}{q} : p \in \mathcal{P}_{r-1}(\mathbb{F}),\ q \in \mathcal{P}_r(\mathbb{F}) \right\}, \tag{1.12}$$

where $\mathcal{P}_r(\mathbb{F})$ denotes polynomials of degree r with coefficients in the field $\mathbb{F}$. There is a surjective mapping between state-space transfer functions (1.11) and elements of $\mathcal{R}_r(\mathbb{F})$; hence for any rational function $H_r \in \mathcal{R}_r(\mathbb{F})$ we can nonuniquely identify a state-space system with matrices $\mathbf{A} \in \mathbb{F}^{r\times r}$, and $\mathbf{b}, \mathbf{c} \in \mathbb{F}^r$ whose transfer function is H_r. Not all elements of $\mathcal{R}_r(\mathbb{F})$ are members of $\mathcal{H}_2$. For $H_r \in \mathcal{R}_r(\mathbb{F})$ to be in $\mathcal{H}_2$ all its poles must lie in the open left half plane; we denote this space as

$$\mathcal{R}_r^+(\mathbb{F}) \coloneqq \mathcal{R}_r(\mathbb{F}) \cap \mathcal{H}_2 = \left\{ \frac{p}{q} : p \in \mathcal{P}_{r-1}(\mathbb{F}),\ q \in \mathcal{P}_r(\mathbb{F}),\ \text{roots of } q \text{ in LHP} \right\}. \tag{1.13}$$

As many applications of model reduction in science and engineering involve real dynamical systems—e.g., diffuse optimal tomography [19, 39], structural mechanics [25, 43], thermal dynamics [16], and optimal control [25]—here we focus our attention on finding real reduced order models $H_r \in \mathcal{R}_r^+(\mathbb{R})$.

1.2. Advantages. There are two main advantages to our *projected* $\mathcal{H}_2$ (PH2) approach compared to existing methods for $\mathcal{H}_2$-optimal model reduction.

Unlike other $\mathcal{H}_2$-optimal model reduction techniques, PH2 requires only evaluations of the full order model transfer function $H(\mu_j)$—this places minimal requirements on the full order model. In contrast, the iterative rational Krylov algorithm (IRKA) [28] requires a state-space representation of the full order model. Other methods require transfer function derivatives, e.g., transfer function IRKA (TF-IRKA) [6] requires first derivatives and Newton methods [10, 37] require both first and second derivatives. Quadrature-based vector fitting (QuadVF) [23] does not require derivatives but does need a particular limit of H.

PH2 typically yields similar or better reduced order models compared to other techniques while simultaneously using fewer evaluations of the full order model. This is significant because for large-scale models, evaluating $H(z)$ dominates the cost, e.g., if $H(z)$ is the transfer function of a large state-space system

$$\left.\begin{cases} \mathbf{x}'(t) = \mathbf{A}\mathbf{x}(t) + \mathbf{b}u(t), & \mathbf{x}(0) = \mathbf{0} \\ y(t) = \mathbf{c}^*\mathbf{x}(t) \end{cases}\right\}, \quad \text{where} \quad \begin{array}{c} \mathbf{A} \in \mathbb{C}^{n\times n},\ \mathbf{b}, \mathbf{c} \in \mathbb{C}^n, \\ H(z) = \mathbf{c}^*[z\mathbf{I} - \mathbf{A}]^{-1}\mathbf{b}, \end{array} \tag{1.14}$$

then the cost of evaluating $H(z)$ is dominated by the linear solve. As the numerical experiments in section 7 demonstrate, our PH2 approach uses fewer transfer function evaluations than both IRKA and TF-IRKA—often by an order of magnitude. This is because each iteration of PH2 recycles previous evaluations of $H(\mu_j)$, whereas each iteration of standard IRKA and TF-IRKA discards these evaluations and requires $2r$ new evaluations. Similarly, our algorithm tends to find better local minimizers because each inner loop of PH2 solves an overdetermined rational approximation problem where we are able to try multiple initializations. In contrast, the rational interpolant generated by IRKA and TF-IRKA at each step is unique. Compared to QuadVF, both PH2 and QuadVF solve an overdetermined rational approximation but differ in how they approximate the $\mathcal{H}_2$-norm. QuadVF uses a fixed quadrature rule evaluating H on the imaginary axis whereas PH2 projects the $\mathcal{H}_2$-norm as in (1.3) using evaluations of H in the right half plane. As our approximation of the $\mathcal{H}_2$-norm is dynamically chosen, it often yields better reduced order models.

2. Properties of the $\mathcal{H}_2$ Hilbert space.

To begin, we briefly summarize the properties of the $\mathcal{H}_2$ Hilbert space essential for the development of our algorithm.

2.1. Evaluation of $\mathcal{H}_2$ norm. Although the $\mathcal{H}_2$ norm is defined through an integral in (1.1), when H has a state-space representation (1.14) we can compute this norm exactly. In this case the impulse response $h(t)$ and transfer function $H(z)$ are

$$h(t) = \mathbf{c}^* \exp[\mathbf{A}t]\mathbf{b} \qquad \text{and} \qquad H(z) = \mathbf{c}^*[z\mathbf{I} - \mathbf{A}]^{-1}\mathbf{b}. \tag{2.1}$$

Then the $\mathcal{H}_2$ norm can be computed from either the controllability $\mathbf{W}_c$ or observability $\mathbf{W}_o$ Gramians. Both Gramians are the solution to a Lyapunov equation [3, sect. 4.3]:

$$\mathbf{W}_c \coloneqq \int_0^\infty e^{\mathbf{A}t}\mathbf{b}\mathbf{b}^* e^{\mathbf{A}^*t}\,\mathrm{d}t, \qquad \mathbf{A}\mathbf{W}_c + \mathbf{W}_c\mathbf{A}^* = -\mathbf{b}\mathbf{b}^*; \tag{2.2}$$

$$\mathbf{W}_o \coloneqq \int_0^\infty e^{\mathbf{A}^*t}\mathbf{c}\mathbf{c}^* e^{\mathbf{A}t}\,\mathrm{d}t, \qquad \mathbf{A}^*\mathbf{W}_o + \mathbf{W}_o\mathbf{A} = -\mathbf{c}\mathbf{c}^*. \tag{2.3}$$

Using either Gramian, the $\mathcal{H}_2$-norm can be evaluated as [3, eq. (5.28)]

$$\|H\|_{\mathcal{H}_2}^2 \coloneqq \frac{1}{2\pi}\int_{-\infty}^{\infty} |H(\mathrm{i}\omega)|^2\,\mathrm{d}\omega = \int_0^\infty |h(t)|^2\,\mathrm{d}t = \mathbf{c}^*\mathbf{W}_c\mathbf{c} = \mathbf{b}^*\mathbf{W}_o\mathbf{b}. \tag{2.4}$$

2.2. Reproducing kernel Hilbert space. *Reproducing kernel Hilbert spaces* [4] are Hilbert spaces which contain a kernel $K[\mu]$ that is also the sampling operator, i.e., $\langle K[\mu], F\rangle = F(\mu)$. For the $\mathcal{H}_2$ Hilbert space this kernel is $v[\mu]$

$$v[\mu](z) \coloneqq (z+\overline{\mu})^{-1}, \quad \text{where} \quad \mu \in \mathbb{C}_+ \coloneqq \{\mu \in \mathbb{C} : \operatorname{Re}\mu > 0\}. \tag{2.5}$$

The reproducing property follows from the Cauchy integral formula [28, Lem. 2.4]

$$\begin{aligned}\langle v[\mu], H\rangle_{\mathcal{H}_2} &= \frac{1}{2\pi}\int_{-\infty}^{\infty} \overline{v[\mu](\mathrm{i}\omega)}H(\mathrm{i}\omega)d\omega = \frac{1}{2\pi}\int_{-\infty}^{\infty}\frac{1}{-\mathrm{i}\omega+\mu}H(\mathrm{i}\omega)d\omega \\ &= \frac{-1}{2\pi}\int_{-\infty}^{\infty}\frac{1}{\mathrm{i}\omega-\mu}H(\mathrm{i}\omega)d\omega = \frac{-\mathrm{i}}{2\pi}\lim_{R\to\infty}\int_{D_R}\frac{1}{z-\mu}H(z)dz = H(\mu),\end{aligned} \tag{2.6}$$

where D_R denotes the counterclockwise path along the boundary of the right half disk of radius R split along the imaginary axis.

2.3. Meier–Luenberger optimality conditions. The first order optimality conditions for $\mathcal{H}_2$ model reduction by state-space systems are called the *Meier–Luenberger* conditions [36]. These follow from the optimality conditions (1.8) but are frequently presented as Hermite interpolation conditions through use of the reproducing kernel $v[\mu]$. Here we provide a brief derivation under the assumption $H_r \in \mathcal{R}_r^+(\mathbb{C})$ has only simple poles; for a derivation with out this constraint, see [22]. This assumption allows us to parameterize H_r in terms of poles $\boldsymbol{\lambda} \in \mathbb{C}^r$ and residues $\boldsymbol{\rho} \in \mathbb{C}^r$,

$$H_r(z;\boldsymbol{\lambda},\boldsymbol{\rho}) \coloneqq \sum_{k=1}^{r}\frac{\rho_k}{z-\lambda_k} = \sum_{k=1}^{r}\rho_k v[-\overline{\lambda_k}](z), \quad \boldsymbol{\lambda},\boldsymbol{\rho}\in\mathbb{C}^r,\ \lambda_k<0. \tag{2.7}$$

Taking derivatives with respect to the real and imaginary parts yields

$$\frac{\partial}{\partial \operatorname{Re}\lambda_k}\|H-H_r(\cdot;\boldsymbol{\lambda},\boldsymbol{\rho})\|_{\mathcal{H}_2}^2 = \ 2\operatorname{Re}\big\langle\ \rho_k v[-\overline{\lambda_k}]', H-H_r(\cdot;\boldsymbol{\lambda},\boldsymbol{\rho})\big\rangle_{\mathcal{H}_2}; \tag{2.8}$$

$$\frac{\partial}{\partial \operatorname{Im}\lambda_k}\|H-H_r(\cdot;\boldsymbol{\lambda},\boldsymbol{\rho})\|_{\mathcal{H}_2}^2 = -2\operatorname{Re}\big\langle \mathrm{i}\rho_k v[-\overline{\lambda_k}]', H-H_r(\cdot;\boldsymbol{\lambda},\boldsymbol{\rho})\big\rangle_{\mathcal{H}_2}; \tag{2.9}$$

$$\frac{\partial}{\partial \operatorname{Re}\rho_k}\|H-H_r(\cdot;\boldsymbol{\lambda},\boldsymbol{\rho})\|_{\mathcal{H}_2}^2 = -2\operatorname{Re}\big\langle\ v[-\overline{\lambda_k}], H-H_r(\cdot;\boldsymbol{\lambda},\boldsymbol{\rho})\big\rangle_{\mathcal{H}_2}; \tag{2.10}$$

$$\frac{\partial}{\partial \operatorname{Im}\rho_k}\|H-H_r(\cdot;\boldsymbol{\lambda},\boldsymbol{\rho})\|_{\mathcal{H}_2}^2 = -2\operatorname{Re}\big\langle \mathrm{i}v[-\overline{\lambda_k}], H-H_r(\cdot;\boldsymbol{\lambda},\boldsymbol{\rho})\big\rangle_{\mathcal{H}_2}; \tag{2.11}$$

where $v[\mu]'$ denotes the derivative of $v[\mu]$, $v[\mu]'(z) \coloneqq -(z+\overline{\mu})^{-2}$. When these derivatives above are all zero, H_r satisfies the first order necessary conditions. Denoting these parameter values as $\widehat{\boldsymbol{\lambda}}$ and $\widehat{\boldsymbol{\rho}}$, combining terms pairwise, and invoking (2.5) yields

$$0 = \Big\langle v[-\overline{\widehat{\lambda}_k}]', H-H_r(\cdot;\widehat{\boldsymbol{\lambda}},\widehat{\boldsymbol{\rho}})\Big\rangle_{\mathcal{H}_2} \quad \Leftrightarrow \quad H'(-\overline{\widehat{\lambda}_k}) = H_r'(-\overline{\widehat{\lambda}_k};\widehat{\boldsymbol{\lambda}},\widehat{\boldsymbol{\rho}}), \tag{2.12}$$

$$0 = \Big\langle v[-\overline{\widehat{\lambda}_k}], H-H_r(\cdot;\widehat{\boldsymbol{\lambda}},\widehat{\boldsymbol{\rho}})\Big\rangle_{\mathcal{H}_2} \quad \Leftrightarrow \quad H(-\overline{\widehat{\lambda}_k}) = H_r(-\overline{\widehat{\lambda}_k};\widehat{\boldsymbol{\lambda}},\widehat{\boldsymbol{\rho}}), \tag{2.13}$$

provided $|\widehat{\rho}_k| > 0$. These conditions require a locally optimal H_r to be a Hermite interpolant of H at the reflection of the poles $\widehat{\boldsymbol{\lambda}}$ across the imaginary axis. This result applies to real reduced order models as well, since $\mathcal{R}_r^+(\mathbb{R})$ is a subspace of $\mathcal{R}_r^+(\mathbb{C})$,

$$\mathcal{R}_r^+(\mathbb{R}) = \{F \in \mathcal{R}_r^+(\mathbb{C}) : \overline{F(z)} = F(\overline{z})\ \forall z \in \mathbb{C}\}. \tag{2.14}$$

Algorithm 3.1. IRKA (simplified).

Input : FOM system $\{\mathbf{A}, \mathbf{b}, \mathbf{c}\}$, initial interpolation points $\boldsymbol{\mu}^{(0)} = \left[\mu_1^{(0)}, \ldots, \mu_r^{(0)}\right]$
Output : ROM system $\{\mathbf{A}_r, \mathbf{b}_r, \mathbf{c}_r\}$
for $\ell = 0, 1, 2, \ldots$ **do**
  Construct rational Krylov spaces $\mathbf{V}$ and $\mathbf{W}$ given $\boldsymbol{\mu}^{(\ell)}$ using (3.1) and (3.2);
  Build state-space reduced order model $\{\mathbf{A}_r, \mathbf{b}_r, \mathbf{c}_r\}$ with $\mathbf{V}$ and $\mathbf{W}$ via (3.3);
  Choose $\mu_j^{(\ell+1)} = -|\operatorname{Re}\lambda_j| - \mathrm{i}\operatorname{Im}\lambda_j$, where $\{\lambda_j\}_{j=1}^r$ are eigenvalues of $\mathbf{A}_r$;

Further, although this parameterization explicitly excludes higher order poles—i.e., $H_r(z) = (z-\lambda)^{-2}$ cannot be expressed in this parameterization—in practice this is not a concern. Rational functions with higher order poles are nowhere dense in $\mathcal{R}_r^+(\mathbb{C})$ [22, p. 2739] and hence cannot be resolved in finite precision arithmetic.

3. Existing algorithms. There are a variety of techniques for $\mathcal{H}_2$-optimal model reduction. Each of these requires access to different information about the full order model described by H. For example, both IRKA [28] and TF-IRKA [6] are fixed point iterations based on rational interpolants, but IRKA requires access to a state-space representation of H whereas TF-IRKA only requires access to $H(z)$ and $H'(z)$. Van Dooren, Gallivan, and Absil propose a similar fixed point iteration that allows for higher order poles in the reduced order model [21, 22]. There are also Newton methods that require access to $H(z)$, $H'(z)$, and $H''(z)$, such as the approach developed by Meier [37] and a trust-region approach due to Beattie and Gugercin [10]. In addition to these optimal methods, there are also several suboptimal methods that require only access to $H(z)$. For example, QuadVF uses a quadrature rule to approximate the $\mathcal{H}_2$-norm [23] and $\mathcal{H}_2$ pseudooptimality removes the derivative condition from the Meier–Luenberger conditions and finds a reduced order model with fixed poles that minimizes the $\mathcal{H}_2$-norm [44]. In this section we briefly summarize three of these algorithms used as comparisons in section 7: IRKA, TF-IRKA, and QuadVF.

3.1. IRKA. The IRKA [28] builds on earlier work constructing rational interpolants for full order models given in state-space form [27, 45]. Given a state-space system (1.14) with matrices $\mathbf{A}$, $\mathbf{b}$, and $\mathbf{c}$, a Hermite rational interpolant at points $\{\mu_j\}_{j=1}^r$ can be constructed using rational Krylov spaces $\mathcal{W}$ and $\mathcal{V}$,

$$\mathcal{V} = \operatorname{Range}(\mathbf{V}) = \operatorname{Span}\{[\mu_1\mathbf{I} - \mathbf{A}]^{-1}\mathbf{b}, \ldots, [\mu_r\mathbf{I} - \mathbf{A}]^{-1}\mathbf{b}\}, \qquad \mathbf{V}^*\mathbf{V} = \mathbf{I}; \tag{3.1}$$

$$\mathcal{W} = \operatorname{Range}(\mathbf{W}) = \operatorname{Span}\{[\mu_1\mathbf{I} - \mathbf{A}]^{-*}\mathbf{c}, \ldots, [\mu_r\mathbf{I} - \mathbf{A}]^{-*}\mathbf{c}\}, \qquad \mathbf{W}^*\mathbf{W} = \mathbf{I}. \tag{3.2}$$

Then the reduced order model $H_r(z) = \mathbf{c}_r^*[z\mathbf{I} - \mathbf{A}_r]^{-1}\mathbf{b}_r$ with matrices

$$\mathbf{A}_r = (\mathbf{W}^*\mathbf{V})^{-1}\mathbf{W}^*\mathbf{A}\mathbf{V}, \quad \mathbf{b}_r = (\mathbf{W}^*\mathbf{V})^{-1}\mathbf{W}^*\mathbf{b}, \quad \mathbf{c}_r = \mathbf{V}^*\mathbf{c} \tag{3.3}$$

satisfies the Hermite interpolation conditions at each μ_j [28, Cor. 2.2]

$$H(\mu_j) = H_r(\mu_j), \quad H'(\mu_j) = H_r'(\mu_j), \quad j = 1, \ldots, r, \tag{3.4}$$

provided $\mathbf{W}^*\mathbf{V}$ is invertible. This interpolant satisfies the Meier–Luenberger conditions when the poles of H_r—the eigenvalues $\{\lambda_j\}_{j=1}^r$ of $\mathbf{A}_r$—are the interpolation points flipped across the imaginary axis, i.e., $\{-\overline{\lambda_j}\}_{j=1}^r = \{\mu_j\}_{j=1}^r$.

IRKA is a fixed point iteration that uses this Hermite interpolant to find a state-space reduced order model satisfying the Meier–Luenberger conditions. As summarized in Algorithm 3.1, given a set of interpolation points $\{\mu_j\}_{j=1}^r$ IRKA constructs a

Hermite rational interpolant using (3.3) and then the poles of this rational interpolant $\{\lambda_j\}_{j=1}^r$ provide the new interpolation points for the next step, $\mu_j = -\overline{\lambda}_j$. When this iteration converges, the reduced order model $\widehat{H}_r$ satisfies the Meier–Luenberger conditions; moreover $\widehat{H}_r$ is a local minimizer as local maximizers are repellent [7, sect. 7.4.2]. Although IRKA often converges in practice, there are only limited cases where convergence is guaranteed [24] and examples exist where this fixed point iteration does not converge [7, sect. 7.4.2]. For large-scale model reduction, the cost of IRKA is dominated by the linear solves in (3.1) and (3.2). There are several modifications to IRKA that mitigate the cost of these linear solves by, for example, using inexact linear solves [8, 9], recycling information between iterations [1], and constructing local approximations of the full order model [17].

3.2. TF-IRKA. A critical limitation of IRKA is the need for a state-space representation of H for constructing the rational Krylov subspaces $\mathcal{V}$ and $\mathcal{W}$ used to build the rational interpolant reduced order model. TF-IRKA [6] removes this constraint by constructing the reduced order model using a Loewner based approach following the work of Anderson and Antoulas [2]. Given a set of interpolation points $\{\mu_j\}_{j=1}^r$, TF-IRKA builds a Hermite interpolant $H_r(z) = \mathbf{c}_r^*[z\mathbf{E}_r - \mathbf{A}_r]^{-1}\mathbf{b}_r$ using evaluations of $H(\mu_j)$ and its derivative $H'(\mu_j)$ where

$$[\mathbf{A}_r]_{j,k} = \begin{cases} -\frac{\mu_j H(\mu_j) - \mu_k H(\mu_k)}{\mu_j - \mu_k}, & j \neq k; \\ -[zH(z)]'|_{z=\mu_j}, & j = k; \end{cases} \quad [\mathbf{E}_r]_{j,k} = \begin{cases} -\frac{H(\mu_j) - H(\mu_k)}{\mu_j - \mu_k}, & j \neq k; \\ -H'(\mu_j), & j = k; \end{cases} \tag{3.5}$$

and $[\mathbf{b}_r]_j = [\mathbf{c}_r]_j = H(\mu_j)$; here $[\mathbf{A}]_{j,k}$ denotes the j,kth entry of $\mathbf{A}$. Then, as in IRKA, the interpolation points are updated in a fixed point iteration based on the poles of H_r, here the generalized eigenvalues λ of $(\mathbf{A}_r, \mathbf{E}_r)$, e.g., $\mathbf{A}_r\mathbf{x} = \lambda\mathbf{E}_r\mathbf{x}$. When H has a state-space representation, the iterations of IRKA and TF-IRKA are identical in exact arithmetic.

3.3. QuadVF. An alternative approach taken by QuadVF [23] is to approximate the $\mathcal{H}_2$-norm using a quadrature rule and then solve the resulting weighted least squares rational approximation problem. QuadVF uses the Boyd/Clenshaw–Curtis quadrature rule [14] using n evaluations of H plus its limit at $\pm\infty$ and includes a scaling parameter $L > 0$,

$$\|H\|_{\mathcal{H}_2}^2 = \frac{1}{2\pi}\int_{-\infty}^{\infty} |H(\mathrm{i}\omega)|^2 \,\mathrm{d}\omega \approx \frac{|M_+[H]|^2 + |M_-[H]|^2}{4L(n+1)} + \sum_{j=1}^{n} w_j |H(z_j)|^2, \tag{3.6}$$

$$w_j = \frac{L}{2(n+1)\sin^2(j\pi/(n+1))}, \; z_j = \mathrm{i}L\cot\left(\frac{j\pi}{n+1}\right), \; M_\pm[H] = \lim_{\omega\to\pm\infty} \mathrm{i}\omega H(i\omega). \tag{3.7}$$

This yields a diagonally weighted least squares rational approximation problem:

$$\min_{H_r \in \mathcal{R}_r^+(\mathbb{R})} \left\| \begin{bmatrix} \sqrt{w_1} & & & & \\ & \ddots & & & \\ & & \sqrt{w_n} & & \\ & & & \sqrt{w_+} & \\ & & & & \sqrt{w_-} \end{bmatrix} \left(\begin{bmatrix} H(z_1) \\ \vdots \\ H(z_n) \\ M_+[H] \\ M_-[H] \end{bmatrix} - \begin{bmatrix} H_r(z_1) \\ \vdots \\ H_r(z_n) \\ M_+[H_r] \\ M_-[H_r] \end{bmatrix} \right) \right\|_2 ; \; w_\pm = \frac{1}{4L(n+1)}. \tag{3.8}$$

A modified vector fitting [29] constructs a rational approximation in barycentric form minimizing (3.8) by iteratively updating the nodes of the barycentric representation. Although QuadVF will necessarily yield reduced order models that do not satisfy the Meier–Luenberger conditions due to the discretization of the $\mathcal{H}_2$-norm, this technique frequently yields reduced order models with small residual norm $\|H - H_r\|_{\mathcal{H}_2}$.

4. Projected nonlinear least squares. Our approach for $\mathcal{H}_2$-optimal model reduction extends the *projected nonlinear least squares* framework introduced by Hokanson for finite-dimensional problems [31]. In its original presentation, given a nonlinear least squares problem

$$\min_{\boldsymbol{\theta}\in\mathbb{R}^q} \|\mathbf{f}(\boldsymbol{\theta}) - \widetilde{\mathbf{y}}\|_2^2, \qquad \mathbf{f}:\mathbb{R}^q \to \mathbb{C}^n, \tag{4.1}$$

this framework solves a series of projected problems (cf. [31, eq. (2)]):

$$\boldsymbol{\theta}^\ell \coloneqq \operatorname*{argmin}_{\boldsymbol{\theta}\in\mathbb{R}^q} \|\mathbf{P}_{\mathcal{W}_\ell}[\mathbf{f}(\boldsymbol{\theta}) - \mathbf{y}]\|_2^2 = \operatorname*{argmin}_{\boldsymbol{\theta}\in\mathbb{R}^q} \|\mathbf{W}_\ell^*[\mathbf{f}(\boldsymbol{\theta}) - \mathbf{y}]\|_2^2, \tag{4.2}$$

where $\mathbf{P}_{\mathcal{W}_\ell}$ is an orthogonal projector onto $\mathcal{W}_\ell \subset \mathbb{C}^n$ with orthonormal basis $\mathbf{W}_\ell \in \mathbb{C}^{n\times m_\ell}$ so that $\mathbf{P}_{\mathcal{W}_\ell} = \mathbf{W}_\ell\mathbf{W}_\ell^*$. Then by choosing subspaces $\mathcal{W}_\ell$ such that the largest subspace angle between $\mathcal{W}_\ell$ and the range of the Jacobian of $\mathbf{f}(\boldsymbol{\theta}^\ell)$ is small, we obtain an accurate solution the original problem (4.1). The advantage of this approach is that at each step we solve a nonlinear least squares problem of small dimension $m_\ell \ll n$. A caveat though is we must be able to evaluate the inner product $\mathbf{W}_\ell^*\mathbf{f}(\boldsymbol{\theta})$ inexpensively.

Applying this framework to $\mathcal{H}_2$-optimal model reduction converts an infinite-dimensional optimization problem into a sequence of finite-dimensional nonlinear least squares problems. Here the reproducing kernel structure of $\mathcal{H}_2$ provides the requisite inexpensive inner product. In the following subsections we build the projector for the $\mathcal{H}_2$ problem (subsection 4.1) and apply Lemma 1.1 to identify the desired range of the projector (subsection 4.2). Since our choice of projector precludes exact containment, we quantify the error introduced in terms of the subspace angle (subsection 4.3) and show this error can be made arbitrarily small (subsection 4.4).

4.1. Projection. Here we construct the projector $P(\boldsymbol{\mu})$ to be an orthogonal projector onto the subspace $\mathcal{V}(\boldsymbol{\mu})$ that spans the kernel vectors $v[\mu_k]$ (2.5):

$$\mathcal{V}(\boldsymbol{\mu}) \coloneqq \operatorname{Span}\{v[\mu_k]\}_{k=1}^n \subset \mathcal{H}_2, \quad \boldsymbol{\mu} \in \mathbb{C}_+^n \coloneqq \{\mathbf{z}\in\mathbb{C}^n \,|\, \operatorname{Re} z_k > 0\}. \tag{4.3}$$

To build this projector, we first define the linear operator $V(\boldsymbol{\mu}) : \mathbb{C}^n \to \mathcal{V}(\boldsymbol{\mu}) \subset \mathcal{H}_2$ and its adjoint $V(\boldsymbol{\mu})^* : \mathcal{H}_2 \to \mathbb{C}^n$,

$$V(\boldsymbol{\mu})\mathbf{c} = \sum_{k=1}^n c_k v[\mu_k], \quad V(\boldsymbol{\mu})^* H = \begin{bmatrix} \langle v[\mu_1], H\rangle_{\mathcal{H}_2} \\ \vdots \\ \langle v[\mu_n], H\rangle_{\mathcal{H}_2} \end{bmatrix} = \begin{bmatrix} H(\mu_1) \\ \vdots \\ H(\mu_n) \end{bmatrix} =: H(\boldsymbol{\mu}). \tag{4.4}$$

Above we have invoked the kernel identity (2.6) to evaluate the adjoint. These two operators $V(\boldsymbol{\mu})$ and $V(\boldsymbol{\mu})^*$ satisfy the adjoint identity:

$$\langle V(\boldsymbol{\mu})\mathbf{c}, H\rangle_{\mathcal{H}_2} = \sum_{k=1}^n \overline{c_k}\langle v[\mu_k], H\rangle_{\mathcal{H}_2} = \mathbf{c}^* H(\boldsymbol{\mu}) = \langle \mathbf{c}, V(\boldsymbol{\mu})^* H\rangle_{\mathbb{C}^n}. \tag{4.5}$$

We now construct the orthogonal projector $P(\boldsymbol{\mu}) : \mathcal{H}_2 \to \mathcal{V}(\boldsymbol{\mu})$ as

$$P(\boldsymbol{\mu}) \coloneqq V(\boldsymbol{\mu})[V(\boldsymbol{\mu})^* V(\boldsymbol{\mu})]^{-1} V(\boldsymbol{\mu})^* = V(\boldsymbol{\mu})\mathbf{M}(\boldsymbol{\mu})^{-1} V(\boldsymbol{\mu})^*, \tag{4.6}$$

where $\mathbf{M}(\boldsymbol{\mu})$ is the positive definite Cauchy matrix

$$[\mathbf{M}(\boldsymbol{\mu})]_{j,k} \coloneqq \langle v[\mu_j], v[\mu_k]\rangle_{\mathcal{H}_2} = (\mu_j + \overline{\mu_k})^{-1}. \tag{4.7}$$

With these definitions, the projected norm can be evaluated as a weighted Euclidean norm of the difference between samples of H and H_r evaluated at $\boldsymbol{\mu}$:

$$\begin{aligned}\|P(\boldsymbol{\mu})[H-H_r]\|_{\mathcal{H}_2}^2 &= \langle V(\boldsymbol{\mu})\mathbf{M}(\boldsymbol{\mu})^{-1}V(\boldsymbol{\mu})^*[H-H_r],[H-H_r]\rangle_{\mathcal{H}_2}\\ &= \langle \mathbf{M}(\boldsymbol{\mu})^{-\frac{1}{2}}V(\boldsymbol{\mu})^*[H-H_r],\mathbf{M}(\boldsymbol{\mu})^{-\frac{1}{2}}V(\boldsymbol{\mu})^*[H-H_r]\rangle_{\mathcal{H}_2}\\ &= \langle \mathbf{M}(\boldsymbol{\mu})^{-\frac{1}{2}}[H(\boldsymbol{\mu})-H_r(\boldsymbol{\mu})],\mathbf{M}(\boldsymbol{\mu})^{-\frac{1}{2}}[H(\boldsymbol{\mu})-H_r(\boldsymbol{\mu})]\rangle_{\mathbb{C}^n}\\ &= \|\mathbf{M}(\boldsymbol{\mu})^{-\frac{1}{2}}[H(\boldsymbol{\mu})-H_r(\boldsymbol{\mu})]\|_2^2,\end{aligned} \tag{4.8}$$

where $\mathbf{M}(\boldsymbol{\mu})^{-\frac{1}{2}}$ is the Hermitian square root of $\mathbf{M}(\boldsymbol{\mu})^{-1}$. Although analytically convenient, computationally we use Cholesky decomposition described in subsection 6.5 in place of $\mathbf{M}(\boldsymbol{\mu})^{-\frac{1}{2}}$.

4.2. First order necessary conditions. We now revisit Lemma 1.1 to derive conditions under which a local optimizer of the projected problem is also a local optimizer of the original problem. For simplicity we consider a parameterization of $\mathcal{R}_r^+(\mathbb{C})$ in terms of poles and residues (cf. (2.7)):

$$\widehat{\boldsymbol{\lambda}},\widehat{\boldsymbol{\rho}} \coloneqq \operatorname*{argmin}_{\substack{\boldsymbol{\lambda},\boldsymbol{\rho}\in\mathbb{C}^r\\ \operatorname{Re}\lambda_k<0}} \|H-H_r(\cdot;\boldsymbol{\lambda},\boldsymbol{\rho})\|_{\mathcal{H}_2}^2, \quad H_r(z;\boldsymbol{\lambda},\boldsymbol{\rho}) \coloneqq \sum_{k=1}^r \rho_k v[-\overline{\lambda_k}](z). \tag{4.9}$$

As $\boldsymbol{\lambda}$ and $\boldsymbol{\rho}$ are contained in an open set, we can apply Lemma 1.1. Thus if $\widehat{\boldsymbol{\lambda}},\widehat{\boldsymbol{\rho}}$ are local optimizers of the projected version of (4.9), and $P(\boldsymbol{\mu}) \supseteq \mathcal{T}(\widehat{\boldsymbol{\lambda}},\widehat{\boldsymbol{\rho}})$, where $\mathcal{T}(\widehat{\boldsymbol{\lambda}},\widehat{\boldsymbol{\rho}})$ contains the derivatives with respect to this parameterization,

$$\mathcal{T}(\boldsymbol{\lambda},\boldsymbol{\rho}) \coloneqq \operatorname{Span}\left\{\rho_k v[-\overline{\lambda_k}]', i\rho_k v[-\overline{\lambda_k}]', v[-\overline{\lambda_k}], iv[-\overline{\lambda_k}]\right\}_{k=1}^r \subset \mathcal{H}_2, \tag{4.10}$$

then $\widehat{\boldsymbol{\lambda}},\widehat{\boldsymbol{\rho}}$ are also local optimizers of the original problem (4.9). Note these the vectors in $\mathcal{T}(\boldsymbol{\lambda},\boldsymbol{\rho})$ are precisely those that appear in the derivation the Meier–Luenberger conditions in (2.8)–(2.11). As the span contains all linear combinations, we denote this subspace using $\boldsymbol{\lambda}$ alone,

$$\mathcal{T}(\boldsymbol{\lambda}) \coloneqq \operatorname{Span}\{v[-\overline{\lambda_j}], v[-\overline{\lambda_j}]'\}_{j=1}^r \supseteq \mathcal{T}(\boldsymbol{\lambda},\boldsymbol{\rho}) \tag{4.11}$$

with equality holding when $\rho_k \neq 0$. Finally, as $\mathcal{R}_r^+(\mathbb{R}) \subset \mathcal{R}_r^+(\mathbb{C})$, satisfying $P(\boldsymbol{\mu}) \supseteq \mathcal{T}(\boldsymbol{\lambda})$ is sufficient to apply Lemma 1.1 for $\mathcal{R}_r^+(\mathbb{R})$.

4.3. Approximating necessary conditions. Unfortunately the construction of projector $P(\boldsymbol{\mu})$ precludes exactly satisfying the containment $\operatorname{Range} P(\boldsymbol{\mu}) \supseteq \mathcal{T}(\boldsymbol{\lambda})$; $\mathcal{T}(\boldsymbol{\lambda})$ contains not only $v[-\overline{\lambda}_k]$, but $v[-\overline{\lambda}_k]'$ which is not in the range of $P(\boldsymbol{\mu})$. However, if the range of $P(\boldsymbol{\mu})$ approximates $\mathcal{T}(\boldsymbol{\lambda})$ as measured by the subspace angle we are able to approximately satisfy the necessary conditions for the original problem.

4.3.1. Defining subspace angles. Subspace angles on $\mathcal{H}_2$ are analogously defined to the finite-dimensional case. Given two finite-dimensional subspaces $\mathcal{X} \subset \mathcal{H}_2$ and $\mathcal{Y} \subset \mathcal{H}_2$ of dimension m and n, the kth subspace angle ϕ_k between these subspaces $\mathcal{X}$ and $\mathcal{Y}$ is (cf. [12, eq. (2)])

$$\cos\phi_k(\mathcal{X},\mathcal{Y}) \coloneqq \max_{\substack{X\in\mathcal{X}\\ \|X\|_{\mathcal{H}_2}=1\\ \langle X_j,X\rangle_{\mathcal{H}_2}=0\\ j<k}} \max_{\substack{Y\in\mathcal{Y}\\ \|Y\|_{\mathcal{H}_2}=1\\ \langle Y_j,Y\rangle_{\mathcal{H}_2}=0\\ j<k}} \langle X,Y\rangle_{\mathcal{H}_2}, \quad \phi_1 \leq \phi_2 \leq \cdots \leq \phi_{\min(m,n)}, \tag{4.12}$$

where $X_k \in \mathcal{X}$ and $Y_k \in \mathcal{Y}$ are the arguments that yield ϕ_k. Given unitary basis operators $B_{\mathcal{X}} : \mathbb{C}^m \to \mathcal{X}$ and $B_{\mathcal{Y}} : \mathbb{C}^n \to \mathcal{Y}$, we can compute the subspace angles via the singular values of a finite-dimensional matrix

$$\cos\phi_k(\mathcal{X},\mathcal{Y}) = \sigma_k(B_{\mathcal{X}}^* B_{\mathcal{Y}}); \quad B_{\mathcal{X}}^* B_{\mathcal{Y}} \in \mathbb{C}^{m\times n}, \tag{4.13}$$

where σ_k denotes the kth singular value in descending order; cf. [12, Thm. 1].

4.3.2. Computing subspace angles. To compute the subspace angle between $\mathcal{T}(\boldsymbol{\lambda})$ and $\mathcal{V}(\boldsymbol{\mu})$ (the range of $P(\boldsymbol{\mu})$) we introduce the orthogonal projector $Q(\boldsymbol{\lambda})$ onto $\mathcal{T}(\boldsymbol{\lambda})$. Defining $V'(\boldsymbol{\mu}) : \mathbb{C}^n \to \mathcal{H}_2$ analogously to $V(\boldsymbol{\mu})$ with $v[\mu]'$ in place of $v[\mu]$,

$$V'(\boldsymbol{\mu})\mathbf{c} \coloneqq \sum_{k=1}^{n} c_k v[\mu_k]', \quad V'(\boldsymbol{\mu})^* H \coloneqq \begin{bmatrix} \langle v[\mu_1]', H\rangle_{\mathcal{H}_2} \\ \vdots \\ \langle v[\mu_n]', H\rangle_{\mathcal{H}_2} \end{bmatrix} = \begin{bmatrix} -H'(\mu_1) \\ \vdots \\ -H'(\mu_n) \end{bmatrix}, \tag{4.14}$$

where the last equality follows from integration by parts. Then we define the projector $Q(\boldsymbol{\lambda}) : \mathcal{H}_2 \to \mathcal{T}(\boldsymbol{\lambda})$ as

$$Q(\boldsymbol{\lambda}) \coloneqq \begin{bmatrix} V(-\overline{\boldsymbol{\lambda}}) & V'(-\overline{\boldsymbol{\lambda}}) \end{bmatrix} \begin{bmatrix} V(-\overline{\boldsymbol{\lambda}})^* V(-\overline{\boldsymbol{\lambda}}) & V(-\overline{\boldsymbol{\lambda}})^* V'(-\overline{\boldsymbol{\lambda}}) \\ V'(-\overline{\boldsymbol{\lambda}})^* V(-\overline{\boldsymbol{\lambda}}) & V'(-\overline{\boldsymbol{\lambda}})^* V'(-\overline{\boldsymbol{\lambda}}) \end{bmatrix}^{-1} \begin{bmatrix} V(-\overline{\boldsymbol{\lambda}})^* \\ V'(-\overline{\boldsymbol{\lambda}})^* \end{bmatrix}. \tag{4.15}$$

We denote this interior matrix as $\widehat{\mathbf{M}}(\boldsymbol{\lambda})$,

$$\widehat{\mathbf{M}}(\boldsymbol{\lambda}) \coloneqq \begin{bmatrix} V(-\overline{\boldsymbol{\lambda}})^* V(-\overline{\boldsymbol{\lambda}}) & V(-\overline{\boldsymbol{\lambda}})^* V'(-\overline{\boldsymbol{\lambda}}) \\ V'(-\overline{\boldsymbol{\lambda}})^* V(-\overline{\boldsymbol{\lambda}}) & V'(-\overline{\boldsymbol{\lambda}})^* V'(-\overline{\boldsymbol{\lambda}}) \end{bmatrix} \in \mathbb{C}^{(2r)\times(2r)}, \tag{4.16}$$

whose blocks are

$$[V\,(-\overline{\boldsymbol{\lambda}})^* V\,(-\overline{\boldsymbol{\lambda}})]_{j,k} = \langle v[-\overline{\lambda_j}]\,, v[-\overline{\lambda_k}]\,\rangle_{\mathcal{H}_2} = -(\overline{\lambda_j} + \lambda_k)^{-1}; \tag{4.17}$$

$$[V\,(-\overline{\boldsymbol{\lambda}})^* V'(-\overline{\boldsymbol{\lambda}})]_{j,k} = \langle v[-\overline{\lambda_j}]\,, v[-\overline{\lambda_k}]'\rangle_{\mathcal{H}_2} = -(\overline{\lambda_j} + \lambda_k)^{-2}; \tag{4.18}$$

$$[V'(-\overline{\boldsymbol{\lambda}})^* V'(-\overline{\boldsymbol{\lambda}})]_{j,k} = \langle v[-\overline{\lambda_j}]', v[-\overline{\lambda_k}]'\rangle_{\mathcal{H}_2} = -2(\overline{\lambda_j} + \lambda_k)^{-3}. \tag{4.19}$$

Then to compute the subspace angle, we define the unitary basis operators for $\mathcal{V}(\boldsymbol{\mu}) = \operatorname{Range} P(\boldsymbol{\mu})$ and $\mathcal{T}(\boldsymbol{\lambda}) = \operatorname{Range} Q(\boldsymbol{\lambda})$,

$$B_{\mathcal{V}(\boldsymbol{\mu})} : \mathbb{C}^n \to \mathcal{V}(\boldsymbol{\mu}), \qquad B_{\mathcal{V}(\boldsymbol{\mu})} \coloneqq V(\boldsymbol{\mu})\mathbf{M}(\boldsymbol{\mu})^{-\frac{1}{2}}, \tag{4.20}$$

$$B_{\mathcal{T}(\boldsymbol{\lambda})} : \mathbb{C}^{2r} \to \mathcal{M}(\boldsymbol{\lambda}), \qquad B_{\mathcal{T}(\boldsymbol{\lambda})} \coloneqq \begin{bmatrix} V(-\overline{\boldsymbol{\lambda}}) & V'(-\overline{\boldsymbol{\lambda}}) \end{bmatrix} \widehat{\mathbf{M}}(\boldsymbol{\lambda})^{-\frac{1}{2}}. \tag{4.21}$$

Then the largest subspace angle between $\mathcal{V}(\boldsymbol{\mu})$ and $\mathcal{T}(\boldsymbol{\lambda})$ is

$$\cos\phi_{\max}(\mathcal{T}(\boldsymbol{\lambda}),\mathcal{V}(\boldsymbol{\mu})) = \sigma_{\min}(B_{\mathcal{V}(\boldsymbol{\mu})}^* B_{\mathcal{T}(\boldsymbol{\lambda})}), \tag{4.22}$$

where $\sigma_{\min}$ denotes the smallest singular value and

$$B_{\mathcal{V}(\boldsymbol{\mu})}^* B_{\mathcal{T}(\boldsymbol{\lambda})} = \mathbf{M}(\boldsymbol{\mu})^{-\frac{1}{2}} \begin{bmatrix} V(\boldsymbol{\mu})^* V(-\overline{\boldsymbol{\lambda}}) & V(\boldsymbol{\mu})^* V'(-\overline{\boldsymbol{\lambda}}) \end{bmatrix} \widehat{\mathbf{M}}(\boldsymbol{\lambda})^{-\frac{1}{2}} \in \mathbb{C}^{n\times(2r)}. \tag{4.23}$$

4.3.3. Necessary conditions. We can use the projector $Q(\boldsymbol{\lambda})$ to provide an alternative interpretation of the optimality conditions (1.8) and (1.6). We first rewrite (1.8) in terms of the projector $Q(\boldsymbol{\lambda})$:

$$\langle H - H_r, T\rangle_{\mathcal{H}_2} = 0 \;\forall T \in \mathcal{T}(\boldsymbol{\lambda}) \;\Leftrightarrow\; \langle H - H_r, Q(\boldsymbol{\lambda})F\rangle_{\mathcal{H}_2} = 0 \quad \forall F \in \mathcal{H}_2\,, \tag{4.24}$$

$$\Leftrightarrow\; \langle Q(\boldsymbol{\lambda})[H - H_r], F\rangle_{\mathcal{H}_2} = 0 \quad \forall F \in \mathcal{H}_2, \tag{4.25}$$

where the second equivalence follows as $Q(\boldsymbol{\lambda})$ is an orthogonal projector. The choice of F that maximizes this second equivalence is $F = Q(\boldsymbol{\lambda})[H - H_r]$ up to a scalar multiple. Hence,

$$\langle H - H_r, T\rangle_{\mathcal{H}_2} = 0 \quad \forall T \in \mathcal{T}(\boldsymbol{\lambda}) \quad \Leftrightarrow \quad \|Q(\boldsymbol{\lambda})[H - H_r]\|_{\mathcal{H}_2} = 0. \tag{4.26}$$

Applying the same argument to the projected problem, the local optimality conditions in (1.8) and (1.6) are equivalently

$$\|Q(\widehat{\boldsymbol{\lambda}})[H - H_r(\cdot;\widehat{\boldsymbol{\lambda}},\widehat{\boldsymbol{\rho}})]\|_{\mathcal{H}_2} = 0 \qquad \text{(original)}, \tag{4.27}$$

$$\|Q(\widehat{\boldsymbol{\lambda}})P(\boldsymbol{\mu})[H - H_r(\cdot;\widehat{\boldsymbol{\lambda}},\widehat{\boldsymbol{\rho}})]\|_{\mathcal{H}_2} = 0 \qquad \text{(projected)}. \tag{4.28}$$

The following theorem generalizes Lemma 1.1 when Range $P(\boldsymbol{\mu}) \not\supseteq \mathcal{T}(\boldsymbol{\lambda})$.

THEOREM 4.1. *Suppose $H_r(\cdot;\widehat{\boldsymbol{\lambda}},\widehat{\boldsymbol{\rho}})$ is a local minimizer of the projected problem with $\|Q(\widehat{\boldsymbol{\lambda}})P(\boldsymbol{\mu})[H - H_r(\cdot;\widehat{\boldsymbol{\lambda}},\widehat{\boldsymbol{\rho}})]\|_{\mathcal{H}_2} = 0$. Then $H_r(\cdot;\widehat{\boldsymbol{\lambda}},\widehat{\boldsymbol{\rho}})$ satisfies the first order optimality conditions for the original problem* (4.9) *with error*

$$\|Q(\widehat{\boldsymbol{\lambda}})[H - H_r(\cdot;\widehat{\boldsymbol{\lambda}},\widehat{\boldsymbol{\rho}})]\|_{\mathcal{H}_2} \le \|H - H_r(\cdot;\widehat{\boldsymbol{\lambda}},\widehat{\boldsymbol{\rho}})\|_{\mathcal{H}_2} \sin\phi_{\max}(\mathcal{V}(\boldsymbol{\mu}),\mathcal{T}(\widehat{\boldsymbol{\lambda}})). \tag{4.29}$$

Proof. Inserting the identity $I = I - P(\boldsymbol{\mu}) + P(\boldsymbol{\mu})$ into the left-hand side we have

$$\begin{aligned}\|Q(\widehat{\boldsymbol{\lambda}})[H - H_r(\cdot;\widehat{\boldsymbol{\lambda}},\widehat{\boldsymbol{\rho}})]\|_{\mathcal{H}_2} \\ \le \|Q(\widehat{\boldsymbol{\lambda}})(I-P(\boldsymbol{\mu}))[H-H_r(\cdot;\widehat{\boldsymbol{\lambda}},\widehat{\boldsymbol{\rho}})]\|_{\mathcal{H}_2}+\|Q(\widehat{\boldsymbol{\lambda}})P(\boldsymbol{\mu})[H-H_r(\cdot;\widehat{\boldsymbol{\lambda}},\widehat{\boldsymbol{\rho}})]\|_{\mathcal{H}_2}.\end{aligned} \tag{4.30}$$

The second term is zero since $H_r(\cdot;\widehat{\boldsymbol{\lambda}},\widehat{\boldsymbol{\rho}})$ satisfies the local optimality conditions of the projected problem in (4.28). Bounding this quantity using the induced $\mathcal{H}_2$-norm yields

$$\|Q(\widehat{\boldsymbol{\lambda}})[H - H_r(\cdot;\widehat{\boldsymbol{\lambda}},\widehat{\boldsymbol{\rho}})]\|_{\mathcal{H}_2} \le \|Q(\widehat{\boldsymbol{\lambda}})(I - P(\boldsymbol{\mu}))\|_{\mathcal{H}_2}\|H - H_r(\cdot;\widehat{\boldsymbol{\lambda}},\widehat{\boldsymbol{\rho}})\|_{\mathcal{H}_2}. \tag{4.31}$$

By definition, the first term on the right is the largest subspace angle between $\mathcal{V}(\boldsymbol{\mu})$ and $\mathcal{T}(\widehat{\boldsymbol{\lambda}})$ [12, eq. (13)],

$$\|Q(\widehat{\boldsymbol{\lambda}})(I - P(\boldsymbol{\mu}))\|_{\mathcal{H}_2} = \sin\phi_{\max}(\mathcal{V}(\boldsymbol{\mu}),\mathcal{T}(\widehat{\boldsymbol{\lambda}})). \tag{4.32}$$

∎

4.4. Finite-difference subspace. Although we cannot have exact containment of $\mathcal{T}(\boldsymbol{\lambda})$ inside $\mathcal{V}(\boldsymbol{\mu})$, we can get arbitrarily close. To provide an intuition of how this can happen, note that as a derivative, $v[\mu]'$ can be approximated by a finite difference for some small complex δ:

$$v[\mu]' \approx \frac{v[\mu+\delta] - v[\mu-\delta]}{2|\delta|} \in \mathcal{V}([\mu-\delta,\mu+\delta]). \tag{4.33}$$

In the same spirit, the following theorem shows that the subspace $\mathcal{V}(\boldsymbol{\mu})$ with μ_j clustering near $-\overline{\lambda}$ can approximate $\mathcal{T}(\boldsymbol{\lambda})$ to arbitrary accuracy. Combined with Theorem 4.1, this theorem shows that local optimizers of the PH2 problem can satisfy the optimality conditions of the original $\mathcal{H}_2$ problem to arbitrary accuracy.

THEOREM 4.2. *Let $\mathcal{V}(\boldsymbol{\mu})$ be an n-dimensional subspace of $\mathcal{H}_2$ with $\boldsymbol{\mu} \in \mathbb{C}_+^n$ as defined in* (4.4) *where $\boldsymbol{\mu}$ are distinct and let $\mathcal{T}(\boldsymbol{\lambda})$ be a $2r$-dimensional subspace of $\mathcal{H}_2$ with $\boldsymbol{\lambda} \in \mathbb{C}_-^r$ as defined in* (4.11) *where $\boldsymbol{\lambda}$ are distinct. If for each λ_k, there exist entries of $\boldsymbol{\mu}$ denoted $\mu_{k,1}$, $\mu_{k,2}$, and $\mu_{k,3}$ where $|\mu_{k,t} + \overline{\lambda_k}| \le \epsilon$ for $t = 1,2,3$ and no entry $\mu_{k,t}$ is repeated, then there exists a constant C independent of ϵ such that*

$$\sin\phi_{\max}(\mathcal{T}(\boldsymbol{\lambda}),\mathcal{V}(\boldsymbol{\mu})) \le C\epsilon. \tag{4.34}$$

A proof is provided in the appendix.

5. Outer loop: Sampling the full order model. Having shown in the previous section that the local optimality conditions can be satisfied to arbitrary accuracy using the projected nonlinear least squares framework, we now design an efficient algorithm constructing a sequence of projectors $\{P(\boldsymbol{\mu}^\ell)\}_{\ell=0}^\infty$ to solve the $\mathcal{H}_2$-optimal model reduction problem. As we assume the dominant cost is evaluating the full order model—namely evaluating $H(z)$—we choose a nested sequence of projectors

$$\text{Range}\, P(\boldsymbol{\mu}^\ell) \subset \text{Range}\, P(\boldsymbol{\mu}^{\ell+1}), \qquad \boldsymbol{\mu}^{\ell+1} \coloneqq \begin{bmatrix} \boldsymbol{\mu}^\ell & \boldsymbol{\mu}_\star^\ell \end{bmatrix}, \tag{5.1}$$

to reuse previous evaluations of $H(\mu_j)$. In this section we provide an effective algorithm for choosing these new interpolation points $\boldsymbol{\mu}_\star^\ell$. However, there are many choices for $\boldsymbol{\mu}_\star^\ell$ that will yield locally optimal models upon convergence as illustrated by the following theorem.

THEOREM 5.1. *Let $H \in \mathcal{H}_2$ and n_0, r be positive integers where $n_0 \geq 2r$. Given an initial $\boldsymbol{\mu}^0 \in \mathbb{C}_+^{n_0}$, let $\boldsymbol{\mu}^{\ell+1} \coloneqq \begin{bmatrix} \boldsymbol{\mu}^\ell & \boldsymbol{\mu}_\star^\ell \end{bmatrix}$ where $\boldsymbol{\mu}_\star^\ell \in \mathbb{C}_+^{n_\ell}$ and the entries of $\boldsymbol{\mu}^\ell$ are distinct for all ℓ. Let $\widehat{H}_r^\ell$ be a locally optimal solution to the projected problem*

$$\widehat{H}_r^\ell \coloneqq \underset{H_r \in \mathcal{R}_r^+(\mathbb{C})}{\text{argmin}} \|P(\boldsymbol{\mu}^\ell)[H - H_r]\|_{\mathcal{H}_2} \text{ with } \|Q(\boldsymbol{\lambda}^\ell)P(\boldsymbol{\mu}^\ell)[H - \widehat{H}_r^\ell]\|_{\mathcal{H}_2} = 0 \tag{5.2}$$

and $\boldsymbol{\lambda}^\ell$ are the poles of $\widehat{H}_r^\ell$. If $\widehat{H}_r^\ell \to \widehat{H}_r \in \mathcal{H}_2$ where $\widehat{H}_r$ has r distinct poles $\boldsymbol{\lambda} \in \mathbb{C}_-^r$ and the sequence $\{\boldsymbol{\mu}_\star^\ell\}_{\ell=0}^\infty$ has limit points $-\overline{\boldsymbol{\lambda}}$, then $\widehat{H}_r$ satisfies the first order necessary conditions of the $\mathcal{H}_2$ problem (4.27)*; i.e., $\widehat{H}_r$ satisfies the Meier–Luenberger conditions.*

Inspired by IRKA, we could satisfy the conditions of this theorem using the poles of the current iterate flipped across the imaginary axis. If $\widehat{H}_r^\ell$ has poles $\boldsymbol{\lambda}^\ell$, then the choice $\boldsymbol{\mu}_\star^\ell = -\overline{\boldsymbol{\lambda}}^\ell$ has the desired limit points as $\boldsymbol{\lambda}^\ell \to \boldsymbol{\lambda}$ if $\widehat{H}_r^\ell \to \widehat{H}_r$ (Lemma A.5). In practice, we desire to use fewer evaluations of the full order model. Hence at each step we add a single new interpolation point; e.g., $\mu_\star^\ell \in \mathbb{C}_+$. Here we describe one effective choice and its practical modifications.

5.1. Selecting interpolation points. As with the IRKA-inspired update, we choose new interpolation points $\mu_\star^\ell$ from the poles of $\widehat{H}_r^\ell$ flipped across the imaginary axis. Specifically we will choose $\mu_\star^\ell$ to be the flipped pole of $\widehat{H}_r^\ell$ that is furthest away from $\mathcal{V}(\boldsymbol{\mu})$ in terms of the subspace angle,

$$\mu_\star^\ell \coloneqq -\overline{\lambda}_\star^\ell, \quad \text{where} \quad \lambda_\star^\ell \coloneqq \underset{\lambda \in \boldsymbol{\lambda}^\ell}{\text{argmax}}\ \sin\phi_{\max}(\mathcal{V}(\boldsymbol{\mu}^\ell), \mathcal{T}(\lambda)), \tag{5.3}$$

where $\boldsymbol{\lambda}^\ell$ are the poles of $\widehat{H}_r^\ell$. Provided these choices of $\lambda_\star^\ell$ do not avoid a particular pole of $\widehat{H}_r^\ell$ asymptotically, then $\{\mu_\star^\ell\}_{\ell=0}^\infty$ has limit points $-\overline{\boldsymbol{\lambda}}$ and this choice satisfies the assumptions of Theorem 5.1. These subspace angles can be computed via (4.22):

$$\cos\phi_{\max}(\mathcal{V}(\boldsymbol{\mu}), \mathcal{T}(\lambda)) = \sigma_{\min}\left(\mathbf{M}(\boldsymbol{\mu})^{-\frac{1}{2}} \begin{bmatrix} \frac{1}{\mu_1 - \lambda} & \frac{1}{(\mu_1 - \lambda)^2} \\ \vdots & \vdots \\ \frac{1}{\mu_n - \lambda} & \frac{1}{(\mu_n - \lambda)^2} \end{bmatrix} \begin{bmatrix} \frac{-1}{\overline{\lambda}+\lambda} & \frac{1}{(\overline{\lambda}+\lambda)^2} \\ \frac{1}{(\overline{\lambda}+\lambda)^2} & \frac{-2}{(\overline{\lambda}+\lambda)^3} \end{bmatrix}^{-\frac{1}{2}}\right). \tag{5.4}$$

Evaluating this subspace angle is inexpensive, taking only $\mathcal{O}(n^2)$ operations, and can reuse the factorization of $\mathbf{M}(\boldsymbol{\mu})$ computed as part of solving the nonlinear least squares problem as discussed in subsection 6.5.

Algorithm 5.1. Projected nonlinear least squares for real $\mathcal{H}_2$ model reduction.

Input : Real FOM $H \in \mathcal{H}_2$, order $r > 0$, initial samples $\boldsymbol{\mu}^0 \in \mathbb{C}_+^{n_0}$, tolerance $\tau > 0$
Output : Real ROM $H_r \in \mathcal{H}_2$

1 **for** $\ell = 0, 1, 2, \ldots$ **do**
2 Set n to be the length of $\boldsymbol{\mu}^\ell$;
3 **if** $n < 2r$ **then** Set $r \leftarrow 2\lfloor n/4 \rfloor$ for only the next iteration;
4 Solve projected problem: $\widehat{H}_r^\ell \leftarrow \operatorname{argmin}_{H_r \in \mathcal{R}_r^+(\mathbb{R})} \|P(\boldsymbol{\mu}^\ell)[H - H_r]\|_{\mathcal{H}_2}$;
5 **if** $\|\widehat{H}_r^\ell - \widehat{H}_r^{\ell-1}\|_{\mathcal{H}_2} < \tau$ **then break**;
6 Compute poles of $\widehat{H}_r^\ell$: $\boldsymbol{\lambda} \leftarrow \lambda(\widehat{H}_r^\ell) \subset \mathbb{C}_-^r$;
7 Using AAA, construct a degree-$(\widehat{r}, \widehat{r})$ rational approximation G of $\boldsymbol{\mu}, H(\boldsymbol{\mu})$;
8 Compute poles of G: $\boldsymbol{\nu} \leftarrow \lambda(G)$; flip into $\mathbb{C}_-^r$ by $\nu_j \leftarrow -|\operatorname{Re}\nu_j| + \mathrm{i}\operatorname{Im}\nu_j$;
9 Order $\boldsymbol{\nu}$ to minimize $|\nu_j - \lambda_j|$ using the Kuhn–Munkres algorithm;
10 **if** $\lambda_j \notin \mathcal{F}(\boldsymbol{\mu})$ **then** set $\lambda_j \leftarrow \nu_j$;
11 Compute furthest pole: $\lambda_\star \leftarrow \operatorname{argmax}_{\lambda \in \boldsymbol{\lambda}} \phi_{\max}(\mathcal{M}(\lambda), \mathcal{V}(\boldsymbol{\mu}))$;
12 **if** $\operatorname{Im}\lambda_\star \neq 0$ **then** Update samples: $\boldsymbol{\mu}^{\ell+1} \leftarrow \begin{bmatrix}\boldsymbol{\mu}^\ell & -\lambda_\star & -\overline{\lambda_\star}\end{bmatrix}$;
13 **else** Update samples: $\boldsymbol{\mu}^{\ell+1} \leftarrow \begin{bmatrix}\boldsymbol{\mu}^\ell & -\lambda_\star\end{bmatrix}$;

5.1.1. When Theorem 5.1 does not hold. A notable case that does not satisfy the assumptions of this theorem occurs when $H \in \mathcal{R}_r^+(\mathbb{R})$. For this case, given any set of distinct samples $\boldsymbol{\mu} \in \mathbb{C}_+^n$ where $n \geq 2r$ we recover H exactly, namely $\widehat{H}_r = H$. Thus the poles of $\widehat{H}_r^\ell$ are always the same and the sequence $\{\mu_\star^\ell\}_{\ell=0}^\infty$ violates the assumption of being distinct. However, in this case, we still obtain an optimal reduced order model.

5.1.2. Improved updates. Before continuing, we note there may be better updates than (5.3). For example, we could choose μ to minimize the subspace angle between the tangent subspace associated with the current iterate and the projection subspace,

$$\min_{\mu \in \mathbb{C}_+} \ \sin \phi_{\max}(\mathcal{T}(\boldsymbol{\lambda}(\widehat{H}_r^\ell)), \mathcal{V}(\boldsymbol{\mu}^\ell) \cup \mathcal{V}(\mu)). \tag{5.5}$$

However, unlike the update rule we propose, this is a nonconvex optimization problem and evaluating these subspace angles is both expensive and ill-conditioned.

5.2. Practical algorithm. In numerical practice, we modify the iteration given in (5.3) as described in Algorithm 5.1 (where AAA is the adaptive Anderson–Antoulas method).

5.2.1. Conjugate samples. Since we assume that the full order model $H \in \mathcal{H}_2$ is real, we can evaluate $H(\mu)$ and $H(\overline{\mu})$ through only one evaluation of H as $\overline{H(\mu)} = H(\overline{\mu})$. Thus if $\mu_\star^\ell$ is not on the real line, we automatically include its conjugate in line 12 which incurs no additional evaluation of H.

5.2.2. Intermediate dimension. If the rational approximation problem is underdetermined, we choose an intermediate dimension for the reduced order model $\widehat{r} < r$ such that the rational approximation problem on line 4 exactly determined or overdetermined. We always pick an even order (cf. line 3) as odd real rational models must have a pole on the real line, but $\widehat{H}_r$ may not.

5.2.3. Spurious poles. The least squares rational approximation step on line 4 may yield a solution whose poles are spurious for our purposes. For example, a pole

may be far away from existing samples, e.g., with $\operatorname{Im}\mu_j \in [-1,1]$, there could be a pole λ_k with $\operatorname{Im}\lambda_k \approx 10^7$ then $(\mu_j - \lambda_k)^{-1}$ is small leading to inaccurate estimation of λ_k. Similarly, a pole λ_k may appear on the imaginary axis with $\operatorname{Re}\lambda_k = 0$, an artifact of the box constraints introduced to ensure $H_r \in \mathcal{H}_2$ (see subsection 6.1). Without modification, a spurious pole can trigger a cascade leading the algorithm to fail: the subspace angle criteria on line 11 ensures these spurious poles are selected, causing $\mathbf{M}(\boldsymbol{\mu})$ to be ill-conditioned and leading subsequent rational approximation steps to fail. To mitigate this failure mode we introduce a heuristic to identify and replace these spurious poles. We label poles as spurious if they fall outside of box containing $\boldsymbol{\mu}$ that has been enlarged by a factor of 10:

$$\mathcal{F}(\boldsymbol{\mu}) \coloneqq \left[-10 \max_{\mu\in\boldsymbol{\mu}} \operatorname{Re}\mu, -0.1 \min_{\mu\in\boldsymbol{\mu}} \operatorname{Re}\mu\right] \times \mathrm{i}\left[10 \min_{\mu\in\boldsymbol{\mu}} \operatorname{Im}\mu, 10 \max_{\mu\in\boldsymbol{\mu}} \operatorname{Im}\mu\right] \subset \mathbb{C}_-. \tag{5.6}$$

Scaling by a factor of 10 balances the need to allow new interpolation points μ to extend beyond existing $\boldsymbol{\mu}$ while still identifying likely spurious poles. When a pole has been labeled spurious, we replace this pole with the corresponding pole from a AAA rational approximation as shown on line 10; note this AAA rational approximation was already constructed during the initialization of the rational approximation step (see subsection 6.4). Although the AAA poles are not optimal, in practice they are not spurious and provide relevant information about H. Although this alters the iteration presented in Theorem 5.1, this result still applies as if $\widehat{H}_r^\ell \to \widehat{H}_r$, eventually all poles lie in $\mathcal{F}(\boldsymbol{\mu})$, and this modification is inactive.

5.2.4. Termination criteria. Here we terminate the algorithm when the difference between subsequent iterates measured in the $\mathcal{H}_2$-norm is small (line 5), choosing this norm to remove the effects of parameterization of H_r. Computing this quantity only requires $\mathcal{O}(r^3)$ operations using (2.4), Ideally based on Theorem 4.1, we would prefer to terminate when the subspace angle between $\mathcal{V}(\boldsymbol{\mu}^\ell)$ and $\mathcal{T}(\boldsymbol{\lambda}(\widehat{H}_r^\ell))$ is sufficiently small; unfortunately this quantity proves difficult to compute accurately.

6. Inner loop: Constructing a reduced order model. A critical component of our PH2 approach is the construction of a *weighted least squares rational approximant* on line 4 of Algorithm 5.1,

$$\widehat{H}_r^\ell \coloneqq \operatorname*{argmin}_{H_r\in\mathcal{R}_r^+(\mathbb{R})} \|P(\boldsymbol{\mu}^\ell)[H - H_r]\|_{\mathcal{H}_2} = \operatorname*{argmin}_{H_r\in\mathcal{R}_r^+(\mathbb{R})} \|\mathbf{M}(\boldsymbol{\mu}^\ell)^{-\frac{1}{2}}[H(\boldsymbol{\mu}^\ell) - H_r(\boldsymbol{\mu}^\ell)]\|_2. \tag{6.1}$$

In Theorem 4.2, an important assumption required for the outer loop to yield local optimizers was that these iterates $\widehat{H}_r^\ell$ are local optimizers of (6.1). Unfortunately, many popular rational fitting algorithms do not yield local optimizers for this problem. For example, AAA [38] exactly interpolates at some μ_j and suboptimally approximates on the remainder. Both the Sanathanan–Koerner iteration [40] and vector fitting [29] have been shown, in general, to converge to rational approximants that do not satisfy the necessary conditions [42]. This lack of existing results motivates our development of a nonlinear least squares approach to solve this weighted rational approximation problem. Here we introduce a two-term partial fraction expansion of H_r to implicitly enforce the constraint that H_r is real and apply variable projection [26] to reduce the dimension of the optimization problem. Additional information about this approach appears in a companion manuscript [32].

6.1. Parameterization. To construct a rational approximation, we must first choose a parameterization of the space of real rational functions of degree $(r-1, r)$: $\mathcal{R}_r^+(\mathbb{R})$. As discussed in [32, sect. 3.4], naive approaches have significant drawbacks: parametrizing $\mathcal{R}_r^+(\mathbb{R})$ as a ratio of monomials rapidly leads to ill-conditioning and a pole-residue parameterization requires additional nonlinear constraints to ensure the rational function has a real representation. Instead, we use a two-term partial fraction expansion following [32, sect. 4.2]:

$$H_r^{\mathrm{PF}}(z;\mathbf{a},\mathbf{b}) \coloneqq \begin{cases} \displaystyle\sum_{k=1}^{\lfloor r/2 \rfloor} \frac{a_{2k}z + a_{2k-1}}{z^2 + b_{2k}z + b_{2k-1}}, & r \text{ even}; \\ \displaystyle\frac{a_r}{z+b_r} + \sum_{k=1}^{\lfloor r/2 \rfloor} \frac{a_{2k}z + a_{2k-1}}{z^2 + b_{2k}z + b_{2k-1}}, & r \text{ odd}; \end{cases} \qquad \mathbf{a},\mathbf{b} \in \mathbb{R}^r. \tag{6.2}$$

This parameterization has several advantages: it is (comparably) numerically stable, requires only $2r$ *real* parameters, and allows us to enforce $H_r^{\mathrm{PF}} \in \mathcal{R}_r^+(\mathbb{R})$ through a box constraint. Recall $H_r^{\mathrm{PF}} \in \mathcal{R}_r^+(\mathbb{R}) \subset \mathcal{H}_2$ if its poles are in the left half plane. As the poles of H_r^{PF} are $-b_{2k}/2 \pm \sqrt{b_{2k}^2/4 - b_{2k+1}}$ (and $-b_r$ if r is odd) it is both necessary and sufficient to require $b_k > 0$ for H_r^{PF} to be in $\mathcal{R}_r^+(\mathbb{R})$.

6.2. Variable projection. Using this parameterization, we construct the rational approximant by solving the rational approximation problem (6.1)

$$\min_{\substack{\mathbf{a},\mathbf{b}\in\mathbb{R}^r \\ b_k>0}} \left\| \mathbf{M}(\boldsymbol{\mu})^{-\frac{1}{2}} [H(\boldsymbol{\mu}) - H_r^{\mathrm{PF}}(\boldsymbol{\mu};\mathbf{a},\mathbf{b})] \right\|_2. \tag{6.3}$$

We write $H_r^{\mathrm{PF}}(\boldsymbol{\mu};\mathbf{a},\mathbf{b})$ as the matrix-vector product $H_r^{\mathrm{PF}}(\boldsymbol{\mu};\mathbf{a},\mathbf{b}) = \boldsymbol{\Theta}(\mathbf{b})\mathbf{a}$ where

$$\boldsymbol{\Theta}(\mathbf{b}) \coloneqq \begin{cases} \begin{bmatrix} \boldsymbol{\Omega}([\mathbf{b}]_{1:2}) & \cdots & \boldsymbol{\Omega}([\mathbf{b}]_{r-1:r}) \end{bmatrix}, & r \text{ even}; \\ \begin{bmatrix} \boldsymbol{\Omega}([\mathbf{b}]_{1:2}) & \cdots & \boldsymbol{\Omega}([\mathbf{b}]_{r-2:r-1}) & (\boldsymbol{\mu}+b_r)^{-1} \end{bmatrix}, & r \text{ odd}; \end{cases} \tag{6.4}$$

$$\boldsymbol{\Omega}\left(\begin{bmatrix} b_1 \\ b_2 \end{bmatrix}\right) \coloneqq \begin{bmatrix} \frac{\mu_1}{\mu_1^2+b_2\mu_1+b_1} & \frac{1}{\mu_1^2+b_2\mu_1+b_1} \\ \vdots & \vdots \\ \frac{\mu_n}{\mu_n^2+b_2\mu_n+b_1} & \frac{1}{\mu_n^2+b_2\mu_n+b_1} \end{bmatrix} \in \mathbb{C}^{n\times 2}. \tag{6.5}$$

This exposes the separable structure of (6.3), which for fixed $\mathbf{b}$ yields a linear least squares problem in $\mathbf{a}$:

$$\min_{\substack{\mathbf{a},\mathbf{b}\in\mathbb{R}^r \\ b_k>0}} \|\mathbf{M}(\boldsymbol{\mu})^{-\frac{1}{2}} [H(\boldsymbol{\mu}) - \boldsymbol{\Theta}(\mathbf{b})\mathbf{a}]\|_2. \tag{6.6}$$

As the objective function involves the complex 2-norm, we recast this as an optimization problem over the real 2-norm by splitting into real and imaginary components,

$$\min_{\substack{\mathbf{a},\mathbf{b}\in\mathbb{R}^r \\ b_k>0}} \left\| \begin{bmatrix} \operatorname{Re}\mathbf{M}(\boldsymbol{\mu})^{-\frac{1}{2}} H(\boldsymbol{\mu}) \\ \operatorname{Im}\mathbf{M}(\boldsymbol{\mu})^{-\frac{1}{2}} H(\boldsymbol{\mu}) \end{bmatrix} - \begin{bmatrix} \operatorname{Re}\mathbf{M}(\boldsymbol{\mu})^{-\frac{1}{2}} \boldsymbol{\Theta}(\mathbf{b}) \\ \operatorname{Im}\mathbf{M}(\boldsymbol{\mu})^{-\frac{1}{2}} \boldsymbol{\Theta}(\mathbf{b}) \end{bmatrix} \mathbf{a} \right\|_2. \tag{6.7}$$

Applying variable projection yields an equivalent optimization problem over $\mathbf{b}$ alone,

$$\min_{\substack{\mathbf{b}\in\mathbb{R}^r \\ b_k>0}} \left\| \left[\mathbf{I} - \begin{bmatrix} \operatorname{Re}\mathbf{M}(\boldsymbol{\mu})^{-\frac{1}{2}} \boldsymbol{\Theta}(\mathbf{b}) \\ \operatorname{Im}\mathbf{M}(\boldsymbol{\mu})^{-\frac{1}{2}} \boldsymbol{\Theta}(\mathbf{b}) \end{bmatrix} \begin{bmatrix} \operatorname{Re}\mathbf{M}(\boldsymbol{\mu})^{-\frac{1}{2}} \boldsymbol{\Theta}(\mathbf{b}) \\ \operatorname{Im}\mathbf{M}(\boldsymbol{\mu})^{-\frac{1}{2}} \boldsymbol{\Theta}(\mathbf{b}) \end{bmatrix}^+ \right] \begin{bmatrix} \operatorname{Re}\mathbf{M}(\boldsymbol{\mu})^{-\frac{1}{2}} H(\boldsymbol{\mu}) \\ \operatorname{Im}\mathbf{M}(\boldsymbol{\mu})^{-\frac{1}{2}} H(\boldsymbol{\mu}) \end{bmatrix} \right\|_2, \tag{6.8}$$

Algorithm 6.1. Residual and Jacobian for real partial fraction parameterization.

Input : Parameters $\mathbf{b} \in \mathbb{R}^r$, factorization $\mathbf{M}(\boldsymbol{\mu}) = \mathbf{PLDL}^*\mathbf{P}^*$ (6.9)
Output : Residual $\underline{\mathbf{r}} \in \mathbb{R}^{2n}$ and Jacobian $\underline{\mathbf{J}} \in \mathbb{R}^{(2n)\times r}$

1 Form $\boldsymbol{\Theta} \leftarrow \boldsymbol{\Theta}(\mathbf{b})$ as given in (6.4);
2 Compute the short form QR decomposition $\underline{\mathbf{QR}} \leftarrow \begin{bmatrix} \operatorname{Re} \mathbf{D}^{-1/2}\mathbf{L}^{-*}\mathbf{P}\boldsymbol{\Theta} \\ \operatorname{Im} \mathbf{D}^{-1/2}\mathbf{L}^{-*}\mathbf{P}\boldsymbol{\Theta} \end{bmatrix}$;
3 Define $\underline{\mathbf{h}} \leftarrow \begin{bmatrix} \operatorname{Re} \mathbf{D}^{-1/2}\mathbf{L}^{-*}\mathbf{P}H(\boldsymbol{\mu}) \\ \operatorname{Im} \mathbf{D}^{-1/2}\mathbf{L}^{-*}\mathbf{P}H(\boldsymbol{\mu}) \end{bmatrix}$;
4 Compute (real) residual $\underline{\mathbf{r}} \leftarrow \underline{\mathbf{h}} - \underline{\mathbf{Q}}\,\underline{\mathbf{Q}}^\top \underline{\mathbf{h}}$;
5 Form complex residual $\mathbf{r} \leftarrow [\underline{\mathbf{r}}]_{1:n} + i[\underline{\mathbf{r}}]_{n+1:2n}$;
6 Compute linear coefficients $\mathbf{a} \leftarrow \underline{\mathbf{R}}^+ \underline{\mathbf{Q}}^\top \underline{\mathbf{h}}$;
7 **for** $k = 1, \ldots, \lfloor r/2 \rfloor$ **do**
8 $\quad \mathbf{d} \leftarrow \boldsymbol{\mu}^2 + b_{2k}\boldsymbol{\mu} + b_{2k-1}$;
9 $\quad [\underline{\mathbf{K}}]_{\cdot,2k-1} \leftarrow [\mathbf{I} - \underline{\mathbf{Q}}\,\underline{\mathbf{Q}}^\top] \begin{bmatrix} \operatorname{Re} \mathbf{D}^{-1/2}\mathbf{L}^{-*}\mathbf{P} \operatorname{diag}(\mathbf{d})^{-2}(a_{2k}\boldsymbol{\mu} + a_{2k-1}) \\ \operatorname{Im} \mathbf{D}^{-1/2}\mathbf{L}^{-*}\mathbf{P} \operatorname{diag}(\mathbf{d})^{-2}(a_{2k}\boldsymbol{\mu} + a_{2k-1}) \end{bmatrix}$;
10 $\quad [\underline{\mathbf{K}}]_{\cdot,2k} \leftarrow [\mathbf{I} - \underline{\mathbf{Q}}\,\underline{\mathbf{Q}}^\top] \begin{bmatrix} \operatorname{Re} \mathbf{D}^{-1/2}\mathbf{L}^{-*}\mathbf{P} \operatorname{diag}(\boldsymbol{\mu}) \operatorname{diag}(\mathbf{d})^{-2}(a_{2k}\boldsymbol{\mu} + a_{2k-1}) \\ \operatorname{Im} \mathbf{D}^{-1/2}\mathbf{L}^{-*}\mathbf{P} \operatorname{diag}(\boldsymbol{\mu}) \operatorname{diag}(\mathbf{d})^{-2}(a_{2k}\boldsymbol{\mu} + a_{2k-1}) \end{bmatrix}$;
11 $\quad [\underline{\mathbf{L}}]_{\cdot,2k-1} \leftarrow \underline{\mathbf{QR}}^{+\top} \begin{bmatrix} \operatorname{Re} \operatorname{diag}(\mathbf{d})^{-2*}\mathbf{P}^*\mathbf{L}^{-1}\mathbf{D}^{-1/2}\mathbf{r} \\ \operatorname{Im} \operatorname{diag}(\mathbf{d})^{-2*}\mathbf{P}^*\mathbf{L}^{-1}\mathbf{D}^{-1/2}\mathbf{r} \end{bmatrix}$;
12 $\quad [\underline{\mathbf{L}}]_{\cdot,2k} \leftarrow \underline{\mathbf{QR}}^{+\top} \begin{bmatrix} \operatorname{Re} \operatorname{diag}(\boldsymbol{\mu}) \operatorname{diag}(\mathbf{d})^{-2*}\mathbf{P}^*\mathbf{L}^{-1}\mathbf{D}^{-1/2}\mathbf{r} \\ \operatorname{Im} \operatorname{diag}(\boldsymbol{\mu}) \operatorname{diag}(\mathbf{d})^{-2*}\mathbf{P}^*\mathbf{L}^{-1}\mathbf{D}^{-1/2}\mathbf{r} \end{bmatrix}$;
13 **if** *r is odd* **then**
14 $\quad [\underline{\mathbf{K}}]_{\cdot,r} \leftarrow [\mathbf{I} - \underline{\mathbf{Q}}\,\underline{\mathbf{Q}}^\top] \begin{bmatrix} \operatorname{Re} \mathbf{D}^{-1/2}\mathbf{L}^{-*}\mathbf{P} \operatorname{diag}(\boldsymbol{\mu} + b_r)^{-2} a_r \\ \operatorname{Im} \mathbf{D}^{-1/2}\mathbf{L}^{-*}\mathbf{P} \operatorname{diag}(\boldsymbol{\mu} + b_r)^{-2} a_r \end{bmatrix}$;
15 $\quad [\underline{\mathbf{L}}]_{\cdot,r} \leftarrow \underline{\mathbf{QR}}^{+\top} \begin{bmatrix} \operatorname{Re} \operatorname{diag}(\boldsymbol{\mu} + b_r)^{-2*}\mathbf{P}^*\mathbf{L}^{-1}\mathbf{D}^{-1/2}\mathbf{r} \\ \operatorname{Im} \operatorname{diag}(\boldsymbol{\mu} + b_r)^{-2*}\mathbf{P}^*\mathbf{L}^{-1}\mathbf{D}^{-1/2}\mathbf{r} \end{bmatrix}$;
16 $\underline{\mathbf{J}} \leftarrow \underline{\mathbf{K}} + \underline{\mathbf{L}}$;

where $^+$ denotes the pseudoinverse. Computationally we replace $\mathbf{M}(\boldsymbol{\mu})^{-\frac{1}{2}}$ with a high accuracy pivoted Cholesky factor described in subsection 6.5. Algorithm 6.1 shows how to construct the residual and Jacobian of (6.8). Note on line 2 we use a column-pivoted and row-sorted QR to improve conditioning; see [30, sect. 19.4].

6.3. Optimization. There are many algorithms for nonlinear least squares problems. Here we use Branch, Coleman, and Li's trust region algorithm [15] as implemented in SciPy's `least_squares` [33] due to its ability to enforce box constraints. This requires the residual and Jacobian of (6.3), which we compute using Algorithm 6.1. When $\underline{\mathbf{R}}$ is not invertible, we terminate the optimization as the rational approximation has degree less than r.

6.4. Initialization. The rational approximation problem often has many local minimizers with large mismatch. To ensure that we find a good local minimizer with small mismatch, at each step we try two initializations of the optimization algorithm to solve projected problem (6.8), keeping the one with smaller mismatch. One initialization uses the poles of the previous iterate when both are of the same dimension. The other initialization uses the AAA algorithm to construct a degree (r, r) rational approximant ignoring the weighting. As these poles will not in general appear in conjugate pairs—a requirement of $\mathcal{R}_r^+(\mathbb{R})$—we use the Kuhn–Munkres algorithm to pair these poles with their nearest conjugate pair, average them, and flip into the left half plane if necessary to find poles of an element of $\mathcal{R}_r^+(\mathbb{R})$.

Algorithm 6.2. Pivoted $\mathbf{LDL}^*$ factorization of $\mathbf{M}(\boldsymbol{\mu})$.

Input : $\boldsymbol{\mu} \in \mathbb{C}^n$ determining $[\mathbf{M}(\boldsymbol{\mu})]_{j,k} = (\mu_j + \overline{\mu_k})^{-1}$
Output : Permutation matrix $\mathbf{P} \in \mathbb{R}^{n\times n}$, lower triangular matrix $\mathbf{L} \in \mathbb{C}^{n\times n}$, and diagonal matrix $\mathbf{D} \in \mathbb{R}^{n\times n}$ such that $\mathbf{M}(\boldsymbol{\mu}) = \mathbf{PLDL}^*\mathbf{P}^*$

$\mathbf{P} = \mathbf{I} \in \mathbb{R}^{n\times n}$;
$\mathbf{s} \leftarrow (\boldsymbol{\mu} + \overline{\boldsymbol{\mu}})^{-1}$;
for $k = 1, \ldots, n$ **do**
  $j \leftarrow \operatorname{argmax}_{j=k,\ldots n} s_j$;
  Permute $\mathbf{P}_{\cdot,k}, \mathbf{P}_{\cdot,j} \leftarrow \mathbf{P}_{\cdot,j}, \mathbf{P}_{\cdot,k}$;
  Permute $\mu_j, \mu_k \leftarrow \mu_k, \mu_j$;
  Permute $s_j, s_k \leftarrow s_k, s_j$;
  $[\mathbf{s}]_{k+1:n} \leftarrow |[\boldsymbol{\mu}]_{k+1:n} - \mu_k|^2 \odot |[\boldsymbol{\mu}]_{k+1:n} + \overline{\mu_k}|^{-2}$
$\mathbf{g} \leftarrow \mathbf{1} \in \mathbb{C}^n$;
for $k = 1, \ldots, n-1$ **do**
  $[\mathbf{D}]_{k,k} \leftarrow \mu_k + \overline{\mu_k}$;
  $[\mathbf{L}]_{k:n,k} \leftarrow [\mathbf{g}]_{k:n} \odot ([\boldsymbol{\mu}]_{k:n} + \overline{\mu_k})^{-1}$;
  $[\mathbf{g}]_{k+1:n} \leftarrow [\mathbf{g}]_{k+1:n} \odot ([\boldsymbol{\mu}]_{k+1:n} - \mu_k) \odot ([\boldsymbol{\mu}]_{k+1:n} + \overline{\mu_k})^{-1}$;
$[\mathbf{D}]_{n,n} \leftarrow (\mu_n + \overline{\mu_n})^{-1}$;
$[\mathbf{L}]_{n,n} \leftarrow g_n$;

6.5. Evaluating the Gram matrix. Cauchy matrices—such as $\mathbf{M}(\boldsymbol{\mu})$ appearing in (6.1)—have a well-deserved reputation for being ill-conditioned. Our application is no exception. As the outer loop converges the entries of $\boldsymbol{\mu}$ become increasingly close and consequently $\mathbf{M}(\boldsymbol{\mu})$ becomes increasingly ill-conditioned. Fortunately the Cauchy matrix structure enables factorizations with high relative accuracy [13, 20] which we can use to accurately compute $\|\mathbf{M}(\boldsymbol{\mu})^{-\frac{1}{2}}\mathbf{z}\|_2$ for any $\mathbf{z} \in \mathbb{C}^n$. Following Demmel [20, Alg. 3], we compute the Cholesky factorization of $\mathbf{M}(\boldsymbol{\mu})$ using Gaussian elimination with complete pivoting,

$$\mathbf{M}(\boldsymbol{\mu}) = \mathbf{PLDL}^*\mathbf{P}^*, \tag{6.9}$$

where $\mathbf{D}$ is a diagonal matrix, $\mathbf{L}$ is lower triangular, and $\mathbf{P}$ is a permutation matrix. As $\mathbf{M}(\boldsymbol{\mu})$ is Hermitian, we can perform the necessary pivoting a priori reducing the computational complexity of this decomposition from $\mathcal{O}(n^3)$ to $\mathcal{O}(n^2)$ operations [20, Alg. 4]. Then we evaluate this norm as

$$\|P(\boldsymbol{\mu})F\|_{\mathcal{H}_2} = \|\mathbf{M}(\boldsymbol{\mu})^{-\frac{1}{2}}F(\boldsymbol{\mu})\|_2 = \|\mathbf{D}^{-\frac{1}{2}}\mathbf{L}^{-*}\mathbf{P}F(\boldsymbol{\mu})\|_2 \quad \forall F \in \mathcal{H}_2. \tag{6.10}$$

For completeness, Algorithm 6.2 describes how to compute this high relative accuracy Cholesky factorization where $\odot$ denotes the Hadamard (entrywise) product.

7. Numerical experiments. Here we present numerical experiments comparing our PH2 approach to IRKA, TF-IRKA, and QuadVF. Following the principles of reproducible science, our code implementing these algorithms and generating the figures is available at https://github.com/jeffrey-hokanson/SYSMOR.

7.1. Test problems. Systems with oscillatory behavior prove challenging for model reduction. Our two test problems have significant oscillatory behavior as illustrated by the large number of peaks in their Bode plots in Figures 7.1 and 7.2.

7.1.1. ISS 1R component. The 1R component of the International Space Station is a standard test problem for model reduction [18, sect. 2.11] with a sparse

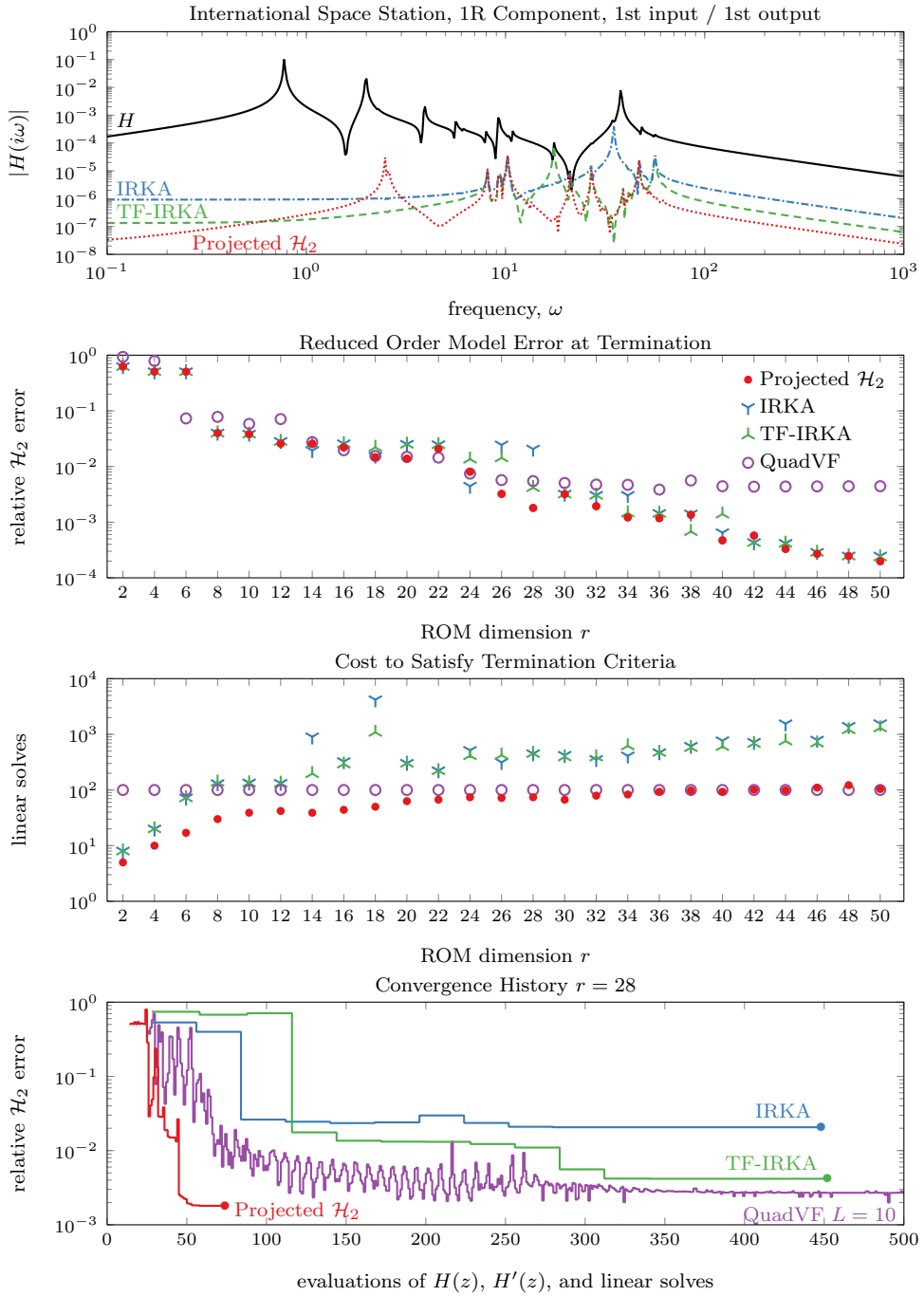

FIG. 7.1. *A comparison of model reduction techniques applied the* 1*R component of the International Space Station described in* [18, *sect.* 2.11]. *The top plot shows the modulus of the transfer function along the imaginary axis, with the broken lines showing the value of the error system* $H - H_r$ *for different techniques at* $r = 28$. *The second plot shows the relative* $\mathcal{H}_2$ *error for each method for a variety of reduced order model dimensions and the table below shows the number of linear solves or, equivalently, evaluations of* $H(z)$ *and* $H'(z)$ *required. The bottom plot shows the convergence history of each of these methods along with a comparison to QuadVF.*

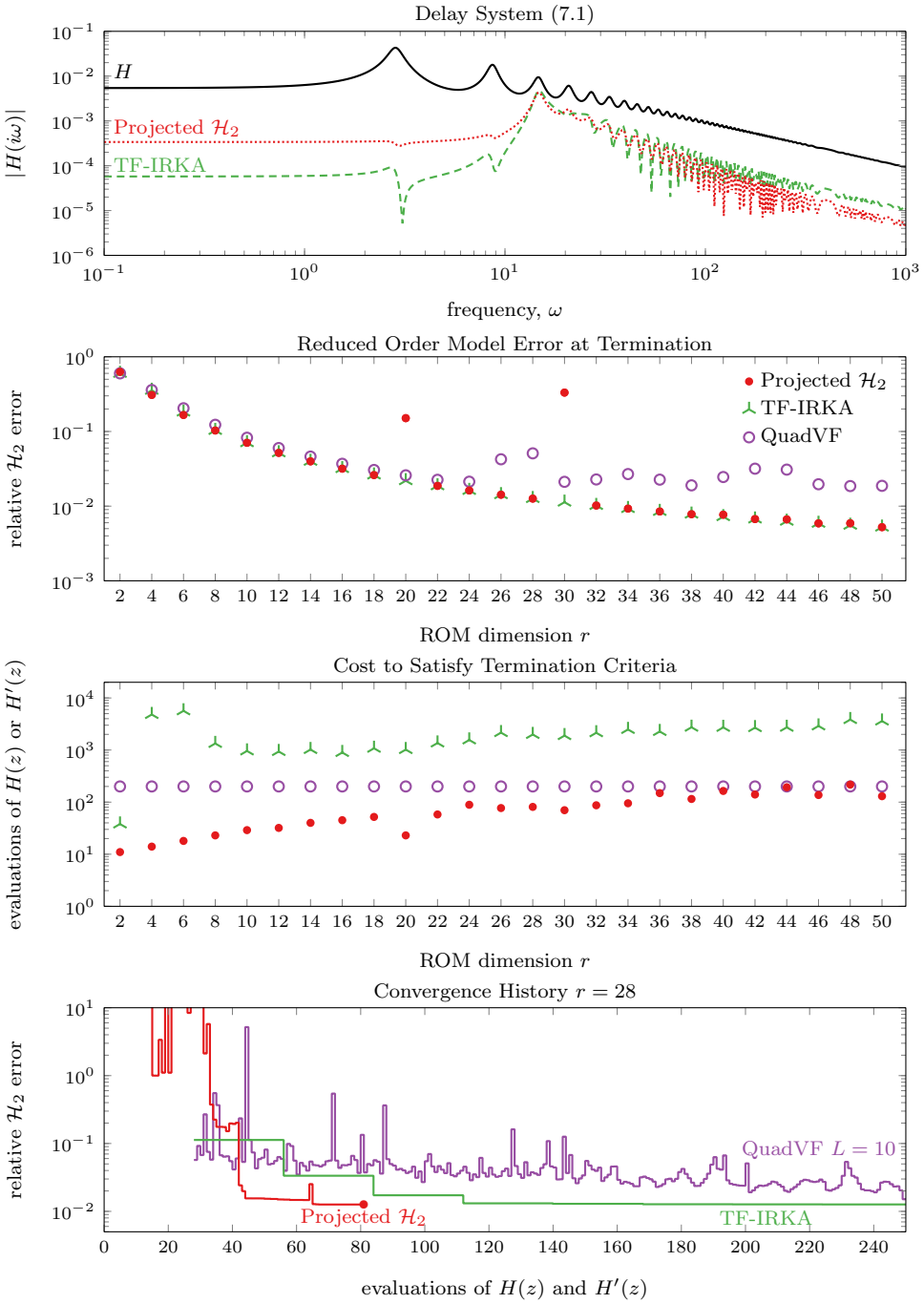

FIG. 7.2. *A comparison of model reduction techniques applied the delay system given in* (7.1). *The top plot shows the modulus of the transfer function along the imaginary axis, with the broken lines showing the value of the error system $H - H_r$ for different techniques at $r = 6$. The second plot shows the relative $\mathcal{H}_2$ error for each method for a variety of reduced order model dimensions and the table below shows the number of evaluations of $H(z)$ and $H'(z)$ required. The bottom plot shows the convergence history of each of these methods. Here we approximate $\mathcal{H}_2$-norm approximately using a Boyd/Clenshaw–Curtis quadrature rule* (3.6) *with* 10^4 *quadrature points.*

state-space representation of dimension 270 with 405 nonzeros. Here we consider the $(1,1)$ block of this transfer function.

7.1.2. Delay system. Here we slightly modify the delay system from [5, sect. 5]:

$$
\begin{aligned}
&H(z) = \mathbf{c}^\top (z\mathbf{E} - \mathbf{A}_0 - e^{-\tau z}\mathbf{A}_1)^{-1}\mathbf{b}, \qquad \text{where} \\
&\mathbf{E} \coloneqq \frac{2}{\sqrt{\epsilon}}\mathbf{I} + \mathbf{T}, \quad \mathbf{A}_0 \coloneqq \frac{2+2\rho}{\tau\rho}\left(\mathbf{T} - \frac{2}{\sqrt{\epsilon}}\mathbf{I}\right), \quad \mathbf{A}_1 \coloneqq \frac{2-2\rho}{\tau\rho}\left(\mathbf{T} - \frac{2}{\sqrt{\epsilon}}\mathbf{I}\right),
\end{aligned} \tag{7.1}
$$

$\mathbf{I} \in \mathbb{R}^{n\times n}$ is the identity matrix and $\mathbf{T} \in \mathbb{R}^{n\times n}$ has ones on the first superdiagonal, the first subdiagonal, and the $(1,1)$ and (n,n) entries and is zero otherwise. Here we choose $n = 1000$, $\tau = 1$, $\rho = 0.1$, $\epsilon = 0.01$, pick $\mathbf{b}$ such that its first two entries are one and the remainder zero, and set $\mathbf{c} = \mathbf{b}$.

7.2. Setup. The performance of each algorithm strongly depends on both the choice of the initialization and the termination conditions. Here we describe how we construct comparable conditions for each algorithm.

7.2.1. Initialization. For PH2, IRKA, and TF-IRKA, each requires an initial set of interpolation points. Following standard practice for IRKA, we choose these interpolation points to be the rightmost r poles of H. For state-space systems, such as the ISS 1R example, these are easily computed from the eigenvalues of $\mathbf{A}$ using an iterative Krylov solver like ARPACK [35]. For the delay example, we computed the poles of H by maximizing $|H(z)|$ starting from pole estimates.

For IRKA and TF-IRKA these r poles provide sufficient data to construct rational interpolants using both transfer function evaluations $H(\mu_j)$ and derivatives $H'(\mu_j)$. However, this same initialization yields an underdetermined rational approximation problem in PH2 as our approach only uses evaluations. Hence, our PH2 approach constructs lower dimensional reduced order models until sufficient data has been accumulated to yield an overdetermined problem. Note that for the $r = 2$, we do not have sufficient data for an even reduced order model and hence use the four rightmost poles of H in this case only.

QuadVF does not need initial shifts, instead taking fixed samples of H along the imaginary axis. However an initialization is still needed for the vector fitting iteration; here we use the poles from AAA as in our PH2 approach. We choose scaling parameter $L = 10$ and set the number of quadrature points to approximately equal the number of evaluations of H used by our PH2 approach at $r = 50$. With $L = 10$ and $N = 100$ the quadrature nodes with positive imaginary part are in $[7.8\times10^{-2}, 6.4\times10^{2}]$i which covers the active region of the Bode plot.

7.2.2. Termination condition. As each algorithm is derived from different principles, each has different natural termination conditions. To provide the same termination condition for each algorithm, we terminate when the difference between successive iterates H_r^ℓ and $H_r^{\ell+1}$ is sufficiently small, namely,

$$
\|H_r^\ell - H_r^{\ell+1}\|_{\mathcal{H}_2} \leq 10^{-9}. \tag{7.2}
$$

This small tolerance is necessary to avoid premature termination and is easily computed in $\mathcal{O}(r^3)$ operations via (2.4).

7.3. Discussion. Figures 7.1 and 7.2 illustrate the performance of several model reduction algorithms on the space station and delay models.

7.3.1. PH2 performance. As these experiments illustrate, our algorithm PH2 often converges to a similar or better local minimizer when compared to IRKA, TF-IRKA, and QuadVF. Moreover, our algorithm always uses fewer evaluations of the transfer function than IRKA and TF-IRKA, often by an order of magnitude. This is not an artifact of the tight termination criteria. As the convergence histories in both examples indicate, the PH2 converges before both IRKA and TF-IRKA have taken their third step. This improved performance is the result of PH2 recycling evaluations of the transfer function between steps whereas IRKA and TF-IRKA must discard previous transfer function evaluations.

7.3.2. Nonmonotonicity in degree. We expect that $\|H - H_r\|_{\mathcal{H}_2}$ should decrease monotonically with increasing degree r as $\mathcal{R}_r^+(\mathbb{R}) \subset \mathcal{R}_{r+1}^+(\mathbb{R})$. This is not necessarily true in our experiments as we can only recover local minimizers—not the global minimizer—since the $\mathcal{H}_2$ model reduction problem is nonconvex.

7.3.3. Nonmonotonicity of iterates. These examples also illustrate that the error $\|H-\widehat{H}_r^\ell\|_{\mathcal{H}_2}$ does not monotonically decrease with iteration ℓ (note evaluations of H effectively count iterations). In PH2 this is unsurprising. Each $\widehat{H}_r^\ell$ is locally optimal with respect to the projection $P(\boldsymbol{\mu}^\ell)$ of the $\mathcal{H}_2$-norm, not the full $\mathcal{H}_2$-norm. In early iterations, the projected norm is a poor approximation of the full norm, leading to inaccurate approximations. This is particularly evident in the delay example.

7.3.4. Oscillation in QuadVF. Both examples show oscillation in the QuadVF $\mathcal{H}_2$ error as we increase the number of quadrature points for a fixed degree as seen in the bottom plot. This is a result of the quadrature rule used to approximate the $\mathcal{H}_2$ norm. When these quadrature nodes are nearby the peaks in the Bode plot we obtain a better fit than when they are far away. Consequently with a large number of quadrature points we are able to find a good approximation; however, prior to that the approximation quality will depend on the location of the quadrature nodes (3.6).

7.3.5. Spurious poles. Finally, we note that PH2 sometimes fails to eliminate spurious poles leading to a larger mismatch than expected. This occurs in the delay example at $r = 20$ and $r = 30$ and illustrates that while the heuristic for removing spurious poles described in subsection 5.2.3 often succeeds, it is not foolproof.

8. Conclusion. We have developed the *projected* $\mathcal{H}_2$ approach for the $\mathcal{H}_2$-optimal model reduction problem by applying the projected nonlinear least squares framework to this problem. This allows the $\mathcal{H}_2$ problem to be converted into a sequence of finite-dimensional rational approximation problems. Although solving these rational approximation problems is more challenging and computationally expensive than constructing rational interpolants as in IRKA and TF-IRKA, this cost is justified by requiring far fewer expensive evaluations of the full order model.

Appendix. We now provide the proofs for Theorems 4.2 and 5.1. A key component in both proofs is the following lemma.

LEMMA A.1. *Let* $f : \mathbb{C}^m \times \mathbb{C}^n \to \mathbb{R}$ *be defined as*

$$f(\mathbf{x},\mathbf{y}) \coloneqq \begin{bmatrix}\mathbf{x}\\ \mathbf{y}\end{bmatrix}^* \begin{bmatrix}\mathbf{A} & \mathbf{B}\\ \mathbf{B}^* & \mathbf{C}\end{bmatrix} \begin{bmatrix}\mathbf{x}\\ \mathbf{y}\end{bmatrix}, \quad \textit{where} \quad \mathbf{A} = \mathbf{A}^*, \mathbf{C} = \mathbf{C}^*, \tag{A.1}$$

and $\mathbf{A}$ *is positive definite; then*

$$\min_{\mathbf{x}\in\mathbb{C}^m} f(\mathbf{x},\mathbf{y}) = \mathbf{y}^*[\mathbf{C} - \mathbf{B}^*\mathbf{A}^{-1}\mathbf{B}]\mathbf{y}. \tag{A.2}$$

Proof. We use Wirtinger calculus (see, e.g., [41, App. A]) that treats $\mathbf{x} \in \mathbb{C}^m$ and its conjugate $\overline{\mathbf{x}}$ as independent variables whose partial derivatives are

$$\frac{\partial \mathbf{x}}{\partial \mathbf{x}} = \mathbf{I}, \qquad \frac{\partial \mathbf{x}}{\partial \overline{\mathbf{x}}} = \mathbf{0}, \qquad \frac{\partial \overline{\mathbf{x}}}{\partial \mathbf{x}} = \mathbf{0}, \qquad \frac{\partial \overline{\mathbf{x}}}{\partial \overline{\mathbf{x}}} = \mathbf{I}. \tag{A.3}$$

Hence the first derivatives of f with respect to $\mathbf{x}$ and $\overline{\mathbf{x}}$ are

$$\frac{\partial f}{\partial \mathbf{x}} = \mathbf{x}^* \mathbf{A} + \mathbf{y}^* \mathbf{B}^* \qquad \frac{\partial f}{\partial \overline{\mathbf{x}}} = \mathbf{x}^\top \mathbf{A}^* + \mathbf{y}^\top \mathbf{B}^\top. \tag{A.4}$$

Setting $\mathbf{x}$ to be $\widehat{\mathbf{x}} = -\mathbf{A}^{-1}\mathbf{B}\mathbf{y}$ makes both derivatives zero; hence $\widehat{\mathbf{x}}$ satisfies the first order necessary conditions. As f is convex in $\mathbf{x}$ as $\mathbf{A}$ is positive definite, the local minimizer $\widehat{\mathbf{x}}$ is the global minimizer. ∎

A.1. Proof of Theorem 4.2. We split this proof into two lemmas that bound terms that later appear in the proof of Theorem 4.2.

LEMMA A.2. *Suppose $\lambda \in \mathbb{C}_-$ and $\mu_1 \in \mathbb{C}_+$ where $|\lambda + \overline{\mu}_1| \leq \epsilon$. Then there exists a constant $C_1 > 0$ independent of ϵ such that*

$$\min_{x_1 \in \mathbb{C}} \|v[-\overline{\lambda}]z_1 + v[\mu_1]x_1\|_{\mathcal{H}_2} \leq |z_1| C_1 \epsilon. \tag{A.5}$$

Proof. Examining the squared objective

$$\|v[-\overline{\lambda}]z_1 + v[\mu_1]x_1\|_{\mathcal{H}_2}^2 = \begin{bmatrix} x_1 \\ z_1 \end{bmatrix}^* \begin{bmatrix} (\mu_1 + \overline{\mu}_1)^{-1} & (\mu_1 - \lambda)^{-1} \\ (-\overline{\lambda} + \overline{\mu}_1)^{-1} & (-\overline{\lambda} - \lambda)^{-1} \end{bmatrix} \begin{bmatrix} x_1 \\ z_1 \end{bmatrix}, \tag{A.6}$$

we note that we can apply Lemma A.1 as $(\mu_1 + \overline{\mu}_1)^{-1}$ is positive. After simplification,

$$\min_{x_1 \in \mathbb{C}} \|v[-\overline{\lambda}]z_1 + v[\mu_1]x_1\|_{\mathcal{H}_2}^2 = |z_1|^2 \frac{|\mu_1 + \overline{\lambda}|^2}{2|\mu_1 - \lambda|^2 \operatorname{Re}[-\lambda]}. \tag{A.7}$$

Setting $\mu_1 = -\overline{\lambda} + \delta$ where $|\delta| \leq \epsilon$ and as $\operatorname{Re}\mu_1 > 0$, $\operatorname{Re}\delta > \operatorname{Re}\lambda$, then

$$|\mu_1 - \lambda| = |-\overline{\lambda} + \delta - \lambda| = |-2\operatorname{Re}\lambda + \delta| \geq |\operatorname{Re}\lambda|. \tag{A.8}$$

Using this bound in the numerator yields the result:

$$\min_{x_1 \in \mathbb{C}} \|v[-\overline{\lambda}]z_1 + v[\mu_1]x_1\|_{\mathcal{H}_2}^2 \leq |z_1|^2 \frac{|\mu_1 + \overline{\lambda}|^2}{2|\operatorname{Re}\lambda|^3} \leq |z_1|^2 C_1^2 \epsilon^2. \tag{A.9}$$ ∎

LEMMA A.3. *Suppose $\lambda \in \mathbb{C}_-$ and $\mu_2, \mu_3 \in \mathbb{C}_+$ where $|\lambda + \overline{\mu}_2| \leq \epsilon$, $|\lambda + \overline{\mu}_3| \leq \epsilon$, and $\mu_2 \neq \mu_3$. Then there exists a constant $C_2 > 0$ independent of ϵ such that*

$$\min_{x_2, x_3 \in \mathbb{C}} \|v[-\overline{\lambda}]' z_2 + v[\mu_2]x_2 + v[\mu_3]x_3\|_{\mathcal{H}_2} \leq |z_2| C_2 \epsilon. \tag{A.10}$$

Proof. Inserting the additive identity $0 = v[\mu_2]' - v[\mu_2]'$ into the objective and applying the triangle inequality

$$\begin{aligned} &\|v[-\overline{\lambda}]' z_2 + v[\mu_2]x_2 + v[\mu_3]x_3\|_{\mathcal{H}_2} \\ &\quad = |z_2| \|v[-\overline{\lambda}]' - v[\mu_2]'\|_{\mathcal{H}_2} + \|v[\mu_2]' z_2 + v[\mu_2]x_2 + v[\mu_3]x_3\|_{\mathcal{H}_2}. \end{aligned} \tag{A.11}$$

The first term above is

$$\|v[-\overline{\lambda}]' - v[\mu_2]'\|_{\mathcal{H}_2}^2 = \frac{2}{(-\overline{\lambda}-\lambda)^3} - \frac{2}{(-\overline{\lambda}+\overline{\mu}_2)^3} - \frac{2}{(\mu_2-\lambda)^3} + \frac{2}{(\mu_2+\overline{\mu}_2)^3}. \tag{A.12}$$

After some simplification and noting $|\lambda - \mu_2| \geq |\operatorname{Re}\lambda|$ following (A.8),

$$\|v[-\overline{\lambda}]' - v[\mu_2]'\|_{\mathcal{H}_2}^2 = 2\frac{|\mu_2+\overline{\lambda}|^2\, p(\mu_2,\lambda,\overline{\mu_2},\overline{\lambda})}{|\lambda-\mu_2|^6 \operatorname{Re}[2\mu_2]^3 \operatorname{Re}[-2\lambda]^3} \leq \frac{|\mu_2+\overline{\lambda}|^2\, p(\mu_2,\lambda,\overline{\mu_2},\overline{\lambda})}{2^5|\operatorname{Re}\lambda|^9 \operatorname{Re}[\mu_2]^3} \leq C_3^2\epsilon^2, \tag{A.13}$$

where $p(\mu_2,\lambda,\overline{\mu_2},\overline{\lambda})$ is a degree-7 polynomial and $C_3 > 0$ captures the terms independent of ϵ. Next, we bound the second term of (A.11); expanding this term

$$\begin{aligned}\|v[\mu_2]x_2 + v[\mu_3]x_3 + v[\mu_2]'z_2\|_{\mathcal{H}_2}^2 \\ = \begin{bmatrix} x_2 \\ x_3 \\ z_2 \end{bmatrix}^* \begin{bmatrix} (\mu_2+\overline{\mu}_2)^{-1} & (\mu_2+\overline{\mu}_3)^{-1} & -(\mu_2+\overline{\mu}_2)^{-2} \\ (\mu_3+\overline{\mu}_2)^{-1} & (\mu_3+\overline{\mu}_3)^{-1} & -(\mu_3+\overline{\mu}_2)^{-2} \\ -(\mu_2+\overline{\mu}_2)^{-2} & -(\mu_2+\overline{\mu}_3)^{-2} & 2(\overline{\mu}_2+\mu_2)^{-3} \end{bmatrix} \begin{bmatrix} x_2 \\ x_3 \\ z_2 \end{bmatrix}.\end{aligned} \tag{A.14}$$

As μ_2 and μ_3 are distinct, the upper left 2×2 block is positive definite and we may apply Lemma A.1 which yields, after some simplification,

$$\min_{x_2,x_3\in\mathbb{C}} \|v[-\overline{\lambda}]'z_2 + v[\mu_2]x_2 + v[\mu_3]x_3\|_{\mathcal{H}_2}^2 = \frac{|z_2|^2|\mu_2-\mu_3|^2}{\operatorname{Re}[2\mu_2]^3|\mu_2+\overline{\mu}_3|^2} \leq C_4^2|z_2|^2\epsilon^2, \tag{A.15}$$

where C_4^2 captures the terms that are independent of ϵ.

Combining (A.13) and (A.15), we obtain the bound

$$\min_{x_2,x_3\in\mathbb{C}} \|v[-\overline{\lambda}]'z_2 + v[\mu_2]x_2 + v[\mu_3]x_3\|_{\mathcal{H}_2} \leq |z_2|\epsilon\sqrt{C_3^2+C_4^2}. \tag{A.16}$$

∎

Proof of Theorem 4.2. We begin by rewriting the sine of the subspace angle in terms of the unitary basis operator $B_{\mathcal{T}(\boldsymbol{\mu})}$ using [12, eq. (13)],

$$\begin{aligned}\sin\phi_{\max}(\mathcal{T}(\boldsymbol{\lambda}),\mathcal{V}(\boldsymbol{\mu})) &= \|(I-P(\boldsymbol{\mu}))B_{\mathcal{T}(\boldsymbol{\lambda})}B_{\mathcal{T}(\boldsymbol{\lambda})}^*\|_{\mathcal{H}_2} \\ &= \max_{\mathbf{y}\in\mathbb{C}^{2r},\|\mathbf{y}\|_2=1} \|(I-P(\boldsymbol{\mu}))B_{\mathcal{T}(\boldsymbol{\lambda})}\mathbf{y}\|_{\mathcal{H}_2}.\end{aligned} \tag{A.17}$$

As $I - P(\boldsymbol{\mu})$ is an orthogonal projector onto the complement of $\mathcal{V}(\boldsymbol{\mu})$, its projection satisfies the closest point property. This permits an equivalent restatement as

$$\sin\phi_{\max}(\mathcal{T}(\boldsymbol{\lambda}),\mathcal{V}(\boldsymbol{\mu})) = \max_{\mathbf{y}\in\mathbb{C}^{2r},\|\mathbf{y}\|_2=1} \min_{\mathbf{x}\in\mathbb{C}^n} \|B_{\mathcal{T}(\boldsymbol{\lambda})}\mathbf{y} + V(\boldsymbol{\mu})\mathbf{x}\|_{\mathcal{H}_2}. \tag{A.18}$$

Writing this in terms of the nonorthogonal basis vectors for $\mathcal{T}(\boldsymbol{\lambda})$ and $\mathcal{V}(\boldsymbol{\mu})$,

$$\sin\phi_{\max}(\mathcal{T}(\boldsymbol{\lambda}),\mathcal{V}(\boldsymbol{\mu})) = \max_{\substack{\mathbf{z}\in\mathbb{C}^{2r} \\ \mathbf{z}\neq 0}} \min_{\mathbf{x}\in\mathbb{C}^n} \frac{\left\| \begin{bmatrix} V(-\overline{\boldsymbol{\lambda}}) & V'(-\overline{\boldsymbol{\lambda}}) \end{bmatrix} \mathbf{z} + V(\boldsymbol{\mu})\mathbf{x} \right\|_{\mathcal{H}_2}}{\|\widehat{\mathbf{M}}(\boldsymbol{\lambda})\mathbf{z}\|_2}. \tag{A.19}$$

We now bound the numerator by making a nonoptimal choice of $\mathbf{x}$. Denoting the entries of $\mathbf{x}$ associated with $\mu_{k,t}$ as $x_{k,t}$ and setting the remainder to zero, we have

$$\min_{\mathbf{x}\in\mathbb{C}^n} \left\| \begin{bmatrix} V(-\overline{\boldsymbol{\lambda}}) & V'(-\overline{\boldsymbol{\lambda}}) \end{bmatrix} \mathbf{z} - V(\boldsymbol{\mu})\mathbf{x} \right\|_{\mathcal{H}_2} \tag{A.20}$$
$$\leq \min_{\substack{\{x_{k,1}\}_{k=1}^m \subset \mathbb{C} \\ \{x_{k,2}\}_{k=1}^m \subset \mathbb{C} \\ \{x_{k,3}\}_{k=1}^m \subset \mathbb{C}}} \left\| \sum_{k=1}^m v[-\overline{\lambda}_k] z_{k,1} + v[-\overline{\lambda}_k]' z_{k,2} + v[\mu_{k,1}] x_{k,1} + v[\mu_{k,2}] x_{k,2} + v[\mu_{k,3}] x_{k,3} \right\|_{\mathcal{H}_2}.$$

Applying the triangle inequality by grouping $v[-\overline{\lambda}_k]$ with $v[\mu_{k,1}]$ and $v'[-\overline{\lambda}_k]$ with $v[\mu_{k,2}]$ and $v[\mu_{k,3}]$ yields the upper bound

$$\begin{aligned} \min_{\mathbf{x}\in\mathbb{C}^n} & \left\| \begin{bmatrix} V(-\overline{\boldsymbol{\lambda}}) & V'(-\overline{\boldsymbol{\lambda}}) \end{bmatrix} \mathbf{z} - V(\boldsymbol{\mu})\mathbf{x} \right\|_{\mathcal{H}_2} \\ & \leq \sum_{k=1}^m \min_{x_{k,1}\in\mathbb{C}} \|v[-\overline{\lambda}_k] z_{k,1} + v[\mu_{k,1}] x_{k,1}\|_{\mathcal{H}_2} \\ & \quad + \sum_{k=1}^m \min_{\substack{x_{k,2}\in\mathbb{C} \\ x_{k,3}\in\mathbb{C}}} \|v[-\overline{\lambda}_k]' z_{k,2} + v[\mu_{k,2}] x_{k,2} + v[\mu_{k,3}] x_{k,3}\|_{\mathcal{H}_2}. \end{aligned} \tag{A.21}$$

In each term, the minimization has been pulled inside the sum as each of $x_{k,1}$ and $x_{k,2}, x_{k,3}$ appear in only one term. Invoking Lemmas A.2 and A.3 we have

$$\min_{\mathbf{x}\in\mathbb{C}^n} \left\| \begin{bmatrix} V(-\overline{\boldsymbol{\lambda}}) & V'(-\overline{\boldsymbol{\lambda}}) \end{bmatrix} \mathbf{z} - V(\boldsymbol{\mu})\mathbf{x} \right\|_{\mathcal{H}_2} \leq \epsilon \sum_{k=1}^m C_{k,1}|z_{k,1}| + C_{k,2}|z_{k,2}|. \tag{A.22}$$

The matrix $\widehat{\mathbf{M}}(\boldsymbol{\lambda})$ is invertible as the entries of $\boldsymbol{\lambda}$ are distinct, which provides the lower bound $\|\widehat{\mathbf{M}}(\boldsymbol{\lambda})\mathbf{z}\|_2 \geq \sigma_{\min}(\widehat{\mathbf{M}}(\boldsymbol{\lambda}))\|\mathbf{z}\|_\infty$. Returning to (A.19) with this lower bound and the upper bound in (A.22),

$$\sin\phi_{\max}(\mathcal{T}(\boldsymbol{\lambda}), \mathcal{V}(\boldsymbol{\mu})) \leq \frac{\epsilon \sum_{k=1}^m C_{k,1}|z_{k,1}| + C_{k,2}|z_{k,2}|}{\sigma_{\min}(\widehat{\mathbf{M}}(\boldsymbol{\lambda}))\|\mathbf{z}\|_\infty} \leq \epsilon \frac{\sum_{k=1}^m C_{k,1} + C_{k,2}}{\sigma_{\min}(\mathbf{M}(\widehat{\boldsymbol{\lambda}}))}, \tag{A.23}$$

where the last step follows from $|z_{k,1}|/\|\mathbf{z}\|_\infty \leq 1$. ∎

A.2. Proof of Theorem 5.1. We begin by establishing a subspace angle result analogous to those in Lemmas A.2 and A.3.

LEMMA A.4. *Suppose $\boldsymbol{\lambda}, \boldsymbol{\xi} \in \mathbb{C}^r$ where $|\lambda_j - \xi_j| \leq \epsilon$. Then there exists a constant $C > 0$ independent of ϵ such that*

$$\sin\phi_{\max}(\mathcal{T}(\boldsymbol{\lambda}), \mathcal{T}(\boldsymbol{\xi})) \leq C\epsilon. \tag{A.24}$$

Proof. As in (A.19), this subspace angle is

$$\sin\phi_{\max}(\mathcal{T}(\boldsymbol{\lambda}), \mathcal{T}(\boldsymbol{\xi})) = \max_{\substack{\mathbf{z}\in\mathbb{C}^{2r} \\ \mathbf{z}\neq 0}} \min_{\mathbf{x}\in\mathbb{C}^{2r}} \frac{\left\| \begin{bmatrix} V(-\overline{\boldsymbol{\lambda}}) & V'(-\overline{\boldsymbol{\lambda}}) \end{bmatrix} \mathbf{z} + \begin{bmatrix} V(-\overline{\boldsymbol{\xi}}) & V'(-\overline{\boldsymbol{\xi}}) \end{bmatrix} \mathbf{x} \right\|_{\mathcal{H}_2}}{\|\widehat{\mathbf{M}}(\boldsymbol{\lambda})\mathbf{z}\|_2}. \tag{A.25}$$

Following (A.21), we make a suboptimal choice of $\mathbf{x}$, pairing those associated with each λ_j and ξ_j and indexing the corresponding entries of $\mathbf{x}$ and $\mathbf{z}$ by $x_{j,1}, x_{j,2}$ and $z_{j,1}, z_{j,2}$:

$$\begin{aligned} \min_{\mathbf{x}\in\mathbb{C}^{2r}} & \left\| \begin{bmatrix} V(-\overline{\boldsymbol{\lambda}}) & V'(-\overline{\boldsymbol{\lambda}}) \end{bmatrix} \mathbf{z} + \begin{bmatrix} V(-\overline{\boldsymbol{\xi}}) & V'(-\overline{\boldsymbol{\xi}}) \end{bmatrix} \mathbf{x} \right\|_{\mathcal{H}_2} \\ & \leq \sum_{j=1}^r \min_{x_{j,1}, x_{j,2}\in\mathbb{C}} \|v[-\overline{\lambda}_j] z_{j,1} + v[-\overline{\lambda}_j]' z_{j,2} + v[-\overline{\xi}_j] x_{j,1} + v[-\overline{\xi}_j]' x_{j,2}\|_{\mathcal{H}_2}. \end{aligned} \tag{A.26}$$

Examining the objective function

(A.27)

$$\begin{aligned}
&\|v[-\overline{\lambda}_j]z_{j,1} + v[-\overline{\lambda}_j]'z_{j,2} + v[-\overline{\xi}_j]x_{j,1} + v[-\overline{\xi}_j]'x_{j,2}\|_{\mathcal{H}_2}^2 \\
&\quad = \begin{bmatrix} z_{j,1} \\ z_{j,2} \\ x_{j,1} \\ x_{j,2} \end{bmatrix}^* \begin{bmatrix} (-\overline{\lambda}_j - \lambda_j)^{-1} & -(-\overline{\lambda}_j - \lambda_j)^{-2} & (-\overline{\lambda}_j - \xi_j)^{-1} & -(-\overline{\lambda}_j - \xi_j)^{-2} \\ -(-\overline{\lambda}_j - \lambda_j)^{-2} & 2(-\overline{\lambda}_j - \lambda_j)^{-3} & -(\overline{\lambda}_j - \xi_j)^{-2} & 2(-\overline{\lambda}_j - \xi_j)^{-3} \\ (-\overline{\xi}_j - \lambda_j)^{-1} & -(-\overline{\xi}_j - \lambda_j)^{-2} & (-\overline{\xi}_j - \xi_j)^{-1} & -(-\overline{\xi}_j - \xi_j)^{-2} \\ -(-\overline{\xi}_j - \lambda_j)^{-2} & 2(-\overline{\xi}_j - \lambda_j)^{-3} & -(\overline{\xi}_j - \xi_j)^{-2} & 2(-\overline{\xi}_j - \xi_j)^{-3} \end{bmatrix} \begin{bmatrix} z_{j,1} \\ z_{j,2} \\ x_{j,1} \\ x_{j,2} \end{bmatrix} \\
&\quad = \begin{bmatrix} \mathbf{z}_j \\ \mathbf{x}_j \end{bmatrix}^* \begin{bmatrix} \widehat{\mathbf{M}}_j & \mathbf{B}_j \\ \mathbf{B}_j^* & \mathbf{C}_j \end{bmatrix} \begin{bmatrix} \mathbf{z}_j \\ \mathbf{x}_j \end{bmatrix}.
\end{aligned}$$

As $\widehat{\mathbf{M}}_j$ is positive definite, we may invoke Lemma A.1 to show

$$\begin{aligned}
\min_{\mathbf{x}_j \in \mathbb{C}^2} &\|v[-\overline{\lambda}_j]z_{j,1} + v[-\overline{\lambda}_j]'z_{j,2} + v[-\overline{\xi}_j]x_{j,1} + v[-\overline{\xi}_j]'x_{j,2}\|_{\mathcal{H}_2}^2 \\
&= \mathbf{z}_j^*[\widehat{\mathbf{M}}_j - \mathbf{B}_j^*\mathbf{C}_j^{-1}\mathbf{B}_j]\mathbf{z}_j.
\end{aligned} \tag{A.28}$$

With this minimizer we bound the squared subspace angle using the singular values

$$\begin{aligned}
\sin^2\phi_{\max}(\mathcal{T}(\boldsymbol{\lambda}), \mathcal{T}(\boldsymbol{\xi})) &\le \max_{\substack{\mathbf{z} \in \mathbb{C}^{2r} \\ \mathbf{z} \neq 0}} \frac{\sum_{j=1}^r \mathbf{z}_j^*[\widehat{\mathbf{M}}_j - \mathbf{B}_j^*\mathbf{C}_j^{-1}\mathbf{B}_j]\mathbf{z}_j}{\mathbf{z}^*\widehat{\mathbf{M}}(\boldsymbol{\lambda})\mathbf{z}} \\
&\le \frac{\sum_{j=1}^r \sigma_{\max}^2(\widehat{\mathbf{M}}_j - \mathbf{B}_j^*\mathbf{C}_j^{-1}\mathbf{B}_j)}{\sigma_{\min}^2(\widehat{\mathbf{M}}(\boldsymbol{\lambda}))}.
\end{aligned} \tag{A.29}$$

Then note the entries of the numerator are all $\mathcal{O}(\epsilon^2)$:

$$[\widehat{\mathbf{M}}_j - \mathbf{B}_j^*\mathbf{C}_j^{-1}\mathbf{B}_j]_{1,1} = \frac{|\lambda_j - \xi_j|^2 p_1(\lambda_j, \xi_j, \overline{\lambda}_j, \overline{\xi}_j)}{3(\lambda_j + \overline{\lambda}_j)^2|\lambda_j + \overline{\xi}_j|^4}; \tag{A.30}$$

$$[\widehat{\mathbf{M}}_j - \mathbf{B}_j^*\mathbf{C}_j^{-1}\mathbf{B}_j]_{1,2} = \frac{|\lambda_j - \xi_j|^2 p_2(\lambda_j, \xi_j, \overline{\lambda}_j, \overline{\xi}_j)}{(\lambda_j + \overline{\lambda}_j)^2(\lambda_j + \overline{\xi}_j)^3(\overline{\lambda}_j + \xi_j)^2}; \tag{A.31}$$

$$[\widehat{\mathbf{M}}_j - \mathbf{B}_j^*\mathbf{C}_j^{-1}\mathbf{B}_j]_{2,2} = \frac{|\lambda_j - \xi_j|^2 p_3(\lambda_j, \xi_j, \overline{\lambda}_j, \overline{\xi}_j)}{3(\lambda_j + \overline{\lambda}_j)^3|\lambda_j + \overline{\xi}_j|^6}, \tag{A.32}$$

where p_1, p_2, and p_3 are all polynomials. As the denominator of (A.29) is independent of ϵ, we obtain the desired bound. ∎

LEMMA A.5. *Suppose $\{\widehat{H}_r^\ell\}_{\ell=0}^\infty \subset \mathcal{R}_r^+(\mathbb{C})$ has a limit $\widehat{H}_r^\ell \to \widehat{H}_r \in \mathcal{R}_r^+(\mathbb{C})$. If $\widehat{H}_r$ has r distinct poles, then the poles $\boldsymbol{\lambda}^\ell$ of $\widehat{H}_r^\ell$ converge to the poles of $\boldsymbol{\lambda}$ of $\widehat{H}_r$.*

Proof. By assumption, we can write $\widehat{H}_r$ in pole-residue form,

$$\widehat{H}_r(z) = \sum_{j=1}^r \rho_j(z - \lambda_j)^{-1}, \quad \text{where} \quad |\rho_j| > 0, \tag{A.33}$$

as otherwise $\widehat{H}_r$ would have fewer than r poles. As rational functions with higher order poles are nowhere dense in $\mathcal{R}_r^+(\mathbb{C})$ [22, p. 2739] and $\widehat{H}_r^\ell \to \widehat{H}_r$ there is some $N > 0$ for which all $\widehat{H}_r^\ell$ with $\ell > N$ has no higher order poles and thus

$$\widehat{H}_r^\ell(z) = \sum_{j=1}^r \rho_j^\ell(z - \lambda_j^\ell)^{-1} \quad \forall \ell > N_1. \tag{A.34}$$

As the pole-residue form is unique up to permutations, then as $\widehat{H}_r^\ell \to \widehat{H}_r$, $\lambda_j^\ell \to \lambda_j$ using an appropriate ordering of λ_j^ℓ. ∎

Proof of Theorem 5.1. We will show that the limit $\widehat{H}_r$ satisfies the first order optimality conditions (4.27), namely $\|Q(\boldsymbol{\lambda})[H - \widehat{H}_r]\|_{\mathcal{H}_2} = 0$, where $\boldsymbol{\lambda}$ denotes the poles of $\widehat{H}_r$.

Beginning by inserting an additive identity $0 = \widehat{H}_r^\ell - \widehat{H}_r^\ell$ and applying the triangle inequality,

$$\|Q(\widehat{\boldsymbol{\lambda}})[H - \widehat{H}_r]\|_{\mathcal{H}_2} \leq \|Q(\widehat{\boldsymbol{\lambda}})[H - \widehat{H}_r^\ell]\|_{\mathcal{H}_2} + \|Q(\widehat{\boldsymbol{\lambda}})[\widehat{H}_r - \widehat{H}_r^\ell]\|_{\mathcal{H}_2}. \tag{A.35}$$

Inserting a multiplicative identity $I = P(\boldsymbol{\mu}^\ell) + [I - P(\boldsymbol{\mu}^\ell)]$ into the first term and again applying the triangle inequality,

$$\|Q(\boldsymbol{\lambda})[H - \widehat{H}_r^\ell]\|_{\mathcal{H}_2} \leq \|Q(\boldsymbol{\lambda})P(\boldsymbol{\mu}^\ell)[H - \widehat{H}_r^\ell]\|_{\mathcal{H}_2} + \|Q(\boldsymbol{\lambda})[I - P(\boldsymbol{\mu}^\ell)][H - \widehat{H}_r^\ell]\|_{\mathcal{H}_2}. \tag{A.36}$$

Once again we insert a multiplicative identity, this time $I = Q(\boldsymbol{\lambda}^\ell) + [I - Q(\boldsymbol{\lambda}^\ell)]$, where $\boldsymbol{\lambda}^\ell$ denotes the poles of $\widehat{H}_r^\ell$ into the first term above, yielding

$$\begin{aligned}\|Q(\boldsymbol{\lambda})P(\boldsymbol{\mu}^\ell)[H - \widehat{H}_r^\ell]\|_{\mathcal{H}_2} \leq{}& \|Q(\boldsymbol{\lambda})Q(\boldsymbol{\lambda}^\ell)P(\boldsymbol{\mu}^\ell)[H - \widehat{H}_r^\ell]\|_{\mathcal{H}_2} \\ &+ \|Q(\boldsymbol{\lambda})[I - Q(\boldsymbol{\lambda}^\ell)]P(\boldsymbol{\mu}^\ell)[H - \widehat{H}_r^\ell]\|_{\mathcal{H}_2}.\end{aligned} \tag{A.37}$$

Since $\widehat{H}_r^\ell$ satisfies the first order optimality conditions, $Q(\boldsymbol{\lambda}^\ell)P(\boldsymbol{\mu}^\ell)[H - \widehat{H}_r^\ell] = 0$ and the first term vanishes. Combining the bounds in (A.35), (A.36), and (A.37)

$$\begin{aligned}\|Q(\boldsymbol{\lambda})[H - \widehat{H}_r]\|_{\mathcal{H}_2} \leq{}& \|Q(\boldsymbol{\lambda})[I - Q(\boldsymbol{\lambda}^\ell)]P(\boldsymbol{\mu}^\ell)[H - \widehat{H}_r^\ell]\|_{\mathcal{H}_2} \\ &+ \|Q(\boldsymbol{\lambda})[I - P(\boldsymbol{\mu}^\ell)][H - \widehat{H}_r^\ell]\|_{\mathcal{H}_2} + \|Q(\boldsymbol{\lambda})[\widehat{H}_r - \widehat{H}_r^\ell]\|_{\mathcal{H}_2}.\end{aligned} \tag{A.38}$$

Then as the induced $\mathcal{H}_2$ norm is submultiplicative and $\|Q(\boldsymbol{\lambda})\|_{\mathcal{H}_2} = 1$,

$$\begin{aligned}\|Q(\boldsymbol{\lambda})[H - \widehat{H}_r]\|_{\mathcal{H}_2} \leq{}& \|Q(\boldsymbol{\lambda})[I - Q(\boldsymbol{\lambda}^\ell)]\|_{\mathcal{H}_2}\|H - \widehat{H}_r^\ell\|_{\mathcal{H}_2} \\ &+ \|Q(\boldsymbol{\lambda})[I - P(\boldsymbol{\mu}^\ell)]\|_{\mathcal{H}_2}\|H - \widehat{H}_r^\ell\|_{\mathcal{H}_2} + \|\widehat{H}_r - \widehat{H}_r^\ell\|_{\mathcal{H}_2}.\end{aligned} \tag{A.39}$$

We now show that each of the terms terms of (A.39) vanishes as $\ell \to \infty$. The first term is multiplied by the subspace angle between the tangent space of $\widehat{H}_r$ and the current iterate $\widehat{H}_r^\ell$:

$$\sin \phi_{\max}(\mathcal{T}(\boldsymbol{\lambda}), \mathcal{T}(\boldsymbol{\lambda}^\ell)) = \|Q(\boldsymbol{\lambda})[I - Q(\boldsymbol{\lambda}^\ell)]\|_{\mathcal{H}_2}. \tag{A.40}$$

By Lemma A.5 we know $\boldsymbol{\lambda}^\ell \to \boldsymbol{\lambda}$ and hence for any $\epsilon > 0$ there is an N_1 such that $|\lambda_j - \lambda_j^\ell| \leq \epsilon$ for all $\ell > N_1$. Then using Lemma A.4 we can show

$$\|Q(\boldsymbol{\lambda})[I - Q(\boldsymbol{\lambda}^\ell)]\|_{\mathcal{H}_2} \leq C_1\epsilon \quad \forall \ell > N_1. \tag{A.41}$$

The second term in (A.39) is multiplied by the subspace angle between the projection subspace and the tangent subspace,

$$\sin \phi_{\max}(\mathcal{T}(\boldsymbol{\lambda}), \mathcal{V}(\boldsymbol{\mu}^\ell)) = \|Q(\boldsymbol{\lambda})[I - P(\boldsymbol{\mu}^\ell)]\|_{\mathcal{H}_2}. \tag{A.42}$$

By assumption $\{\boldsymbol{\mu}_\star^\ell\}_{\ell=0}^\infty$ has limit points $-\overline{\boldsymbol{\lambda}}$. Thus for any $\epsilon > 0$, there exists N_2 such that $|\overline{\lambda}_j^\ell + \mu_{j,t}| \leq \epsilon$ for $t = 1, 2, 3$, where $\mu_{j,t}$ is in $\boldsymbol{\mu}^\ell$. Then invoking Theorem 4.2, there is a constant $C_2 > 0$ such that

$$\|Q(\boldsymbol{\lambda})[I - P(\boldsymbol{\mu}^\ell)]\|_{\mathcal{H}_2} \leq C_2\epsilon \quad \forall \ell > N_2. \tag{A.43}$$

The third term in (A.39) vanishes as by assumption $\widehat{H}_r^\ell \to \widehat{H}_r$. Hence there exists $N_3 > 0$ such that

$$\|\widehat{H}_r^\ell - \widehat{H}_r\|_{\mathcal{H}_2} \leq \epsilon \quad \forall \ell > N_3. \tag{A.44}$$

Finally, we bound (A.39). Using (A.41), (A.43), and (A.44) in (A.39)

$$\|Q(\boldsymbol{\lambda})[H - \widehat{H}_r]\|_{\mathcal{H}_2} \leq \|H - \widehat{H}_r^\ell\|_{\mathcal{H}_2} C_1\epsilon + \|H - \widehat{H}_r^\ell\|_{\mathcal{H}_2} C_2\epsilon + \epsilon \quad \forall \ell > \max\{N_1, N_2, N_3\}. \tag{A.45}$$

Further as $\widehat{H}_r^\ell \to \widehat{H}_r$, there is some C_4 such that

$$\|H - \widehat{H}_r^\ell\| \leq C_4 \quad \forall \ell > N_4. \tag{A.46}$$

Finally, combining these results

$$\|Q(\boldsymbol{\lambda})[H - \widehat{H}_r]\|_{\mathcal{H}_2} \leq [(C_1 + C_2)C_4 + 1]\epsilon. \tag{A.47}$$

As the choice of ϵ was arbitrary, $\|Q(\boldsymbol{\lambda})[H - \widehat{H}_r]\|_{\mathcal{H}_2} = 0$. ∎

Acknowledgments. The authors would like to thank Christopher Beattie, Zlatko Drmač, Mark Embree, Serkan Gugercin, Christian Himpe, Petar Mlinarić, Neeraj Sarna, and the anonymous reviewers for their feedback during the preparation of this manuscript. The first author would also like to thank the Einstein Foundation Berlin and Paul Constantine for their support.

REFERENCES

[1] K. Ahuja, E. de Sturler, S. Gugercin, and E. R. Chang, *Recycling BiCG with an application to model reduction*, SIAM J. Sci. Comput., 34 (2012), pp. A1925–A1949, https://doi.org/10.1137/100801500.

[2] B. D. O. Anderson and A. C. Antoulas, *Rational interpolation and state-variable realizations*, Linear Algebra Appl., 138 (1990), pp. 479–509, https://doi.org/10.1016/0024-3795(90)90140-8.

[3] A. C. Antoulas, *Approximation of Large-Scale Dynamical Systems*, Adv. Des. Control 6, SIAM, Philadelphia, 2005, https://doi.org/10.1137/1.9780898718713.

[4] N. Aronszajn, *Theory of reproducing kernels*, Trans. Amer. Math. Soc., 68 (1950), pp. 337–404, https://doi.org/10.1090/S0002-9947-1950-0051437-7.

[5] C. Beattie and S. Gugercin, *Interpolatory projection methods for structure-preserving model reduction*, Systems Control Lett., 58 (2009), pp. 225–232, https://doi.org/10.1016/j.sysconle.2008.10.016.

[6] C. Beattie and S. Gugercin, *Realization-independent $\mathcal{H}_2$-approximation*, in Proceedings of the 51st Annual Conference on Decision and Control, IEEE, 2012, pp. 4953–4958, https://doi.org/10.1109/CDC.2012.6426344.

[7] C. Beattie and S. Gugercin, *Model reduction by rational interpolation*, in Model Reduction and Approximation, P. Benner, A. Cohen, M. Ohlberger, and K. Wilcox, eds., Comput. Sci. Eng. 15, SIAM, Philadelphia, 2017, pp. 297–334, https://doi.org/10.1137/1.9781611974829.ch7.

[8] C. Beattie, S. Gugercin, and S. Wyatt, *Inexact solves in interpolatory model reduction*, Linear Algebra Appl., 436 (2012), pp. 2916–2943, https://doi.org/10.1016/j.laa.2011.07.015.

[9] C. A. Beattie and S. Gugercin, *Inexact solves in Krylov-based model reduction*, in Proceedings of the 45th IEEE Conference on Decision and Control, IEEE, 2006, pp. 3405–3411, https://doi.org/10.1109/CDC.2006.376798.

[10] C. A. Beattie and S. Gugercin, *A trust region method for optimal $\mathcal{H}_2$ model reduction*, in Proceedings of the Joint 48th IEEE Conference on Decision and Control and 28th Chinese Control Conference, 2009, pp. 5370–5375, https://doi.org/10.1109/CDC.2009.5400605.

[11] P. Benner, A. Cohen, M. Ohlberger, and K. Wilcox, eds., *Model Reduction and Approximation: Theory and Algorithms*, Comput. Sci. Eng. 15, SIAM, Philadelphia, 2017, https://doi.org/10.1137/1.9781611974829.

[12] Å. Björck and G. H. Golub, *Numerical methods for computing angles between linear subspaces*, Math. Comp., 27 (1973), pp. 579–594, https://doi.org/10.1090/S0025-5718-1973-0348991-3.

[13] T. Boros, T. Kailath, and V. Olshevsky, *Pivoting and backwards stability of fast algorithms for solving Cauchy linear equations*, Linear Algebra Appl., 343-344 (2002), pp. 63–99, https://doi.org/10.1016/S0024-3795(01)00519-5.

[14] J. P. Boyd, *Exponentially convergent Fourier-Chebshev quadrature schemes on bounded and infinite intervals*, J. Sci. Comput., 2 (1987), pp. 99–109, https://doi.org/10.1007/BF01061480.

[15] M. A. Branch, T. F. Coleman, and Y. Li, *A subspace, interior, and conjugate gradient method for large-scale bound-constrained minimization problems*, SIAM J. Sci. Comput., 21 (1999), pp. 1–23, https://doi.org/10.1137/S1064827595289108.

[16] T. Bui-Thanh, K. Willcox, and O. Ghattas, *Model reduction for large-scale systems with high-dimensional parametric input space*, SIAM J. Sci. Comput., 30 (2008), pp. 3270–3288, https://doi.org/10.1137/070694855.

[17] A. Castagnotto, H. K. Panzer, and B. Lohmann, *Fast H2-optimal model order reduction exploiting the local nature of Krylov-subspace methods*, in Proceedings of the European Control Conference, IEEE, 2016, pp. 1958–1969, https://doi.org/10.1109/ECC.2016.7810578.

[18] Y. Chahlaoui and P. V. Dooren, *A Collection of Benchmark Examples for Model Reduction of Linear Time Invarant Dynamical Systems*, Tech. report, SLICOT, 2002, http://slicot.org/objects/software/reports/SLWN2002-2.ps.gz.

[19] E. De Sturler, S. Gugercin, M. E. Kilmer, S. Chaturantabut, C. Beattie, and M. O'Connell, *Nonlinear parametric inversion using interpolatory model reduction*, SIAM J. Sci. Comput., 37 (2015), pp. B495–B517, https://doi.org/10.1137/130946320.

[20] J. Demmel, *Accurate singular value decompositions of structured matrices*, SIAM J. Matrix Anal. Appl., 21 (2000), pp. 562–580, https://doi.org/10.1137/S0895479897328716.

[21] P. V. Dooren, K. A. Gallivan, and P.-A. Absil, *$\mathcal{H}_2$-optimal model reduction of MIMO systems*, Appl. Math. Lett., 21 (2008), pp. 1267–1273, https://doi.org/10.1016/j.aml.2007.09.015.

[22] P. V. Dooren, K. A. Gallivan, and P.-A. Absil, *$\mathcal{H}_2$-optimal model reduction with higher-order poles*, SIAM J. Matrix Anal. Appl., 31 (2010), pp. 2738–2753, https://doi.org/10.1137/080731591.

[23] Z. Drmač, S. Gugercin, and C. Beattie, *Quadrature-based vector fitting for discretized $\mathcal{H}_2$ approximation*, SIAM J. Sci. Comput., 37 (2015), pp. A625–A652, https://doi.org/10.1137/140961511.

[24] G. Flagg, C. Beattie, and S. Gugercin, *Convergence of the iterative rational Krylov algorithm*, Systems Control Lett., 61 (2012), pp. 688–691.

[25] W. Gawronski, *Advanced Structural Dynamics and Active Control of Structures*, Springer, New York, 2004.

[26] G. H. Golub and V. Pereyra, *The differentiation of pseudo-inverses and nonlinear least squares problems whose variables separate*, SIAM J. Numer. Anal., 10 (1973), pp. 413–432, https://doi.org/10.1137/0710036.

[27] E. J. Grimme, *Krylov Projection Methods for Model Reduction*, Ph.D. thesis, University of Illinois at Urbana-Champaign, 1997.

[28] S. Gugercin, A. C. Antoulas, and C. Beattie, *$\mathcal{H}_2$ model reduction for large-scale linear dynamical systems*, SIAM J. Matrix Anal. Appl., 30 (2008), pp. 609–638, https://doi.org/10.1137/060666123.

[29] B. Gustavsen and A. Semlyen, *Rational approximation of frequency domain responses by vector fitting*, IEEE Trans. Power Delivery, 14 (1999), pp. 1052–1061, https://doi.org/10.1109/61.772353.

[30] N. J. Higham, *Accuracy and Stability of Numerical Algorithms*, SIAM, Philadelphia, 2002.

[31] J. M. Hokanson, *Projected nonlinear least squares for exponential fitting*, SIAM J. Sci. Comput., 39 (2017), pp. A3107–A3128, https://doi.org/10.1137/16M1084067.

[32] J. M. Hokanson and C. C. Magruder, *Least Squares Rational Approximation*, https://arxiv.org/abs/1811.12590, 2018.
[33] E. Jones, T. Oliphant, P. Peterson, et al., *SciPy: Open Source Scientific Tools for Python*, http://www.scipy.org/.
[34] T. Kato, *Perturbation Theory for Linear Operators*, Springer-Verlag, Berlin, 1995.
[35] R. B. Lehoucq, D. C. Sorensen, and C. Yang, *ARPACK User's Guide: Solution of Large-Scale Eigenvalue Problems with Implicitly Restarted Arnoldi Methods*, Software Environ. Tools 6, SIAM, Philadelphia, 1998, https://doi.org/10.1137/1.9780898719628.
[36] L. Meier and D. Luenberger, *Approximation of linear constant systems*, IEEE Trans. Automat. Control, 12 (1967), pp. 585–588, https://doi.org/10.1109/TAC.1967.1098680.
[37] L. Meier, III, *Approximation of Linear Constant Systems by Linear Constant Systems of Lower Order*, Ph.D. thesis, Stanford University, 1965.
[38] Y. Nakatsukasa, O. Sète, and L. N. Trefethen, *The AAA algorithm for rational approximation*, SIAM J. Sci. Comput., 40 (2018), pp. A1494–A1522, https://doi.org/10.1137/16M1106122.
[39] M. O'Connell, M. E. Kilmer, E. de Sturler, and S. Gugercin, *Computing reduced order models via inner-outer Krylov recycling in diffuse optical tomography*, SIAM J. Sci. Comput., 39 (2017), pp. B272–B297, https://doi.org/10.1137/16M1062880.
[40] C. K. Sanathanan and J. Koerner, *Transfer function synthesis as a ratio of two complex polynomials*, IEEE Trans. Automat. Control, 8 (1963), pp. 56–58, https://doi.org/10.1109/TAC.1963.1105517.
[41] P. J. Schreier and L. L. Scharf, *Statistical Signal Processing of Complex-Valued Data: Theory of Improper and Noncircular Signals*, Cambridge University Press, Cambridge, UK, 2010.
[42] G. Shi, *On the nonconvergence of the vector fitting algorithm*, IEEE Trans. Circuits Syst. II, 63 (2016), pp. 718–722.
[43] T. Stykel and A. Vasilyev, *A two-step model reduction approach for mechanical systems with moving loads*, J. Comput. Appl. Math., 297 (2016), pp. 85–97, https://doi.org/10.1016/j.cam.2015.11.014.
[44] T. Wolf, H. K. F. Panzer, and B. Lohmann, *$\mathcal{H}_2$ pseudo-optimality in model order reduction by Krylov subspace methods*, in Proceedings of the European Control Conference, 2013, pp. 3427–3432, https://doi.org/10.23919/ECC.2013.6669585.
[45] A. Yousuff, D. A. Wagie, and R. E. Skelton, *Linear system approximation via covariance equivalent realizations*, J. Math. Anal. Appl., 106 (1985), pp. 91–115, https://doi.org/10.1016/0022-247X(85)90133-7.